Downloaded from rsta.royalsocietypublishing.org

PHILOSOPHICAL TRANSACTIONS OF THE ROYAL SOCIETY A MATHEMATICAL, PHYSICAL & ENGINEERING SCIENCES

Multicomponent Adsorption in Continuous Countercurrent Exchangers

Hyun-Ku Rhee, R. Aris and N. R. Amundson

Phil. Trans. R. Soc. Lond. A 1971 **269**, 187-215
doi: 10.1098/rsta.1971.0028

Email alerting service

Receive free email alerts when new articles cite this article - sign up in the box at the top right-hand corner of the article or click **here**

To subscribe to *Phil. Trans. R. Soc. Lond. A* go to: **http://rsta.royalsocietypublishing.org/subscriptions**

This journal is © 1971 The Royal Society

Downloaded from rsta.royalsocietypublishing.org

MULTICOMPONENT ADSORPTION IN CONTINUOUS COUNTERCURRENT EXCHANGERS

By HYUN-KU RHEE, R. ARIS, and N. R. AMUNDSON
University of Minnesota

(*Communicated by P. V. Danckwerts, F.R.S.—Received* 20 *March* 1970)

CONTENTS

A theoretical analysis of multicomponent adsorption in continuous countercurrent exchangers is presented. The system is considered to be one-dimensional, isothermal, locally at equilibrium, and to have negligible diffusion effects. With constant initial and entry data the mathematical problem is essentially the same as for a fixed bed except for the boundary condition that suggests a free boundary analogue since it is given by the conservation law itself. Therefore, the boundary discontinuity is naturally encountered. With the Langmuir adsorption isotherm explicit forms for the Riemann invariants and characteristic parameters are available and thus the theories of simple waves and of shock waves as well as of interactions are readily established and applied to determine solutions. Dependence of the system behaviour upon the flow rate ratio is discussed and the steady-state argument proves that the number of steady states attainable in the contacting region is equal to the number of solute species present plus one. Application is illustrated.

Introductory remarks

Continuous operations of adsorption exchangers are desirable from an engineering point of view and are a common subject in chemical engineering text-books (see, for example, Treybal 1968). Prevailing in those are the steady-state analyses for a single solute with a finite resistance to mass

Vol. 269. A. 1194. (Price 16*s*. (£0.8) U.S. $2.05) 13 [Published 5 February 1971

The Royal Society is collaborating with JSTOR to digitize, preserve, and extend access to *Philosophical Transactions of the Royal Society of London. Series A, Mathematical and Physical Sciences.* www.jstor.org

Downloaded from rsta.royalsocietypublishing.org

transfer. An equilibrium model for non-isothermal adsorption was recently suggested by Heerdt (1969), who considered semi-infinite systems with the Langmuir adsorption isotherm. Although the general theory was not discussed, basic features were well explained by presenting illustrative examples for a single solute and two solutes.

We wish in this paper to establish an equilibrium theory of multi-component adsorption in continuous countercurrent exchangers. Since only convective transport is important, the equations of equilibrium exchange form a quasilinear system of partial differential equations of first order. For fixed beds a full discussion has been given by Rhee, Aris & Amundson (1970) and this is the basis of our treatment here. Exchange columns of semi-infinite length as well as of finite length with constant initial and entry data are considered. The relevant boundary conditions are the material balances over each boundary itself and thus a free boundary analogue is encountered.

The first section is concerned with the formulation of basic equations while in the second section we introduce isotherms of Langmuir type and establish the basic theory of simple waves and of shock waves as well as of interactions. The next section treats a semi-infinite column and there the nature of the boundary is observed in detail. The analysis of finite columns is the subject of §4 in which the steady states attainable are also discussed whereas in §5 a complete analysis of interactions is performed. Finally, we consider and illustrate the problem of applying the theory by generating a comprehensive numerical example.

NOTATION

The following are the principal symbols used in this paper. Dimensions are given in terms of mass (M), length (L), time (t), and amount of solute species (mol).

A_i	ith solute species
$A(z)$	cross-sectional area (L^2)
$\mathscr{B}$	boundary
$C^{(k)}$	characteristic of the kth kind
c_i	molar concentration of species A_i in fluid phase (mol/L^3)
D	$1+\sum_{i=1}^{M} K_i c_i$, dimensionless parameter
$J_i^{(k)}$	(k)-Riemann invariant, dimensionless
K_i	Langmuir adsorption isotherm parameter $(mol/L^3)^{-1}$
N	limiting concentration of adsorbed solute (mol/L^3)
n_i	molar concentration of adsorbed A_i (mol/L^3)
Q	volumetric flow rate of fluid phase (L^3/t)
$S^{(k)}$	(k)-shock line
t	time (t)
u	interstitial velocity of fluid phase (L/t)
v	speed of solid phase (L/t)
x	dimensionless position variable
Z	total length of the column (L)
z	distance from the fluid entrance in the direction of fluid flow (L)
$\Gamma^{(k)}$	image of a (k)-simple wave in $\Phi(M)$ or $\Omega(M)$
ϵ	fractional void space of solid phase, dimensionless

Downloaded from rsta.royalsocietypublishing.org

Θ fractional coverage of adsorption sites, dimensionless
$\Lambda_{(k)}$ $\omega_{(k)}D$, dimensionless invariant
μ $(1-\epsilon)v/\epsilon u$, volumetric flow rate ratio, dimensionless
ν $(1-\epsilon)/\epsilon$, volume ratio, dimensionless
$\xi(D)$ inverse of data as a function of D, dimensionless
σ characteristic direction in the physical plane, dimensionless
σ^s direction of shock propagation, dimensionless
τ dimensionless time variable
$\Phi(M)$ M-dimensional concentration space
ϕ_i $K_i c_i$, dimensionless concentration of species A_i in fluid phase
$\Omega(M)$ M-dimensional ω-space
ω characteristic parameter, dimensionless

Brackets

$[a]$ jump of the quantity a across a discontinuity
$\{a_i\}$ collection of M elements a_i associated with the subscript

Superscripts

a entrance of fluid phase
b entrance of solid phase
i initial condition
(k) kth kind or (k)-constant state
l left-hand side of shock
° fixed state
r right-hand side of shock
s shock
0+ inside of the boundary $\mathscr{B}^{\mathrm{a}}$
1− inside of the boundary $\mathscr{B}^{\mathrm{b}}$
* higher value

Subscripts

eq equilibrium value
i,j,k,m solute species in multicomponent systems
(k) kth kind
M total number of solute species or equivalently the most adsorbable species
s.s. steady state
0 initial point
1, 2, 3 solute species A_1, A_2, A_3
* lower value

Underlines

~~~~ constant state

Overlines

— straight line
⌒ curved line
~~~~

Downloaded from rsta.royalsocietypublishing.org

1. Mathematical formulation

Throughout the present work we shall examine in detail what is known as an ideal exchange column where the term 'ideal' will embody the following conditions:

1. The system is one-dimensional in the direction of flow.
2. The volumetric flow rate of each phase and the void fraction of the solid phase are constant.
3. The effect of diffusion is negligible compared with the convective transport and no channelling occurs.
4. Local equilibrium is established between phases everywhere within the contacting region at all times.
5. Adsorption process is isothermal and isochoric.

Let ϵ be the void fraction of the solid phase moving at a speed v through a column of cross-sectional area $A(z)$, whereas the fluid phase flows countercurrently with interstitial velocity u. c_i is the concentration of the species A_i in the fluid phase and n_i its concentration in the solid phase, both being expressed in moles per unit volume of their own phase. A schematic diagram of the ideal column is given in figure 1.

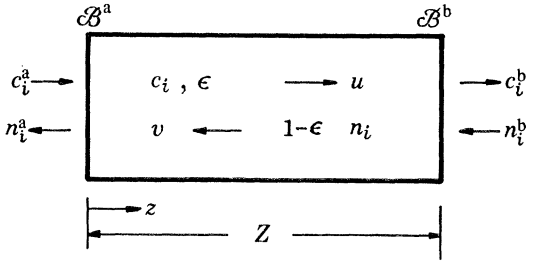

Figure 1. Schematic diagram of an ideal exchange column.

(a) *Continuous field*

By considering the balance of the species A_i in a section between planes distant z and $z+\mathrm{d}z$ from the fluid entrance to the column over a time interval $(t, t+\mathrm{d}t)$ we have, in the limit, the equation

$$Q\left\{\frac{\partial c_i}{\partial z}-\frac{(1-\epsilon)\,v}{\epsilon u}\frac{\partial n_i}{\partial z}\right\}+\epsilon A(z)\left\{\frac{\partial c_i}{\partial t}+\frac{1-\epsilon}{\epsilon}\frac{\partial n_i}{\partial t}\right\}=0 \quad (i=1,2,\ldots,M), \tag{1.1}$$

where

$$Q\equiv \epsilon u(z)\,A(z) = \text{constant volumetric flow rate of the fluid phase.} \tag{1.2}$$

We shall put

$$\nu \equiv \frac{1-\epsilon}{\epsilon} = \text{volume ratio,} \tag{1.3}$$

$$\mu \equiv \frac{1-\epsilon}{\epsilon}\frac{v}{u} = \text{volumetric flow rate ratio,} \tag{1.4}$$

and introduce the dimensionless independent variables defined as

$$x=\int_0^z A(\zeta)\,\mathrm{d}\zeta \Big/ \int_0^Z A(\zeta)\,\mathrm{d}\zeta, \tag{1.5}$$

$$\tau = Qt \Big/ \int_0^Z A(\zeta)\,\mathrm{d}\zeta, \tag{1.6}$$

Downloaded from rsta.royalsocietypublishing.org

in which Z denotes the total length of the column, so that equation (1.1) may be rewritten in the form

$$\frac{\partial}{\partial x}(c_i-\mu n_i)+\epsilon\frac{\partial}{\partial \tau}(c_i+\nu n_i)=0 \quad (i=1,2,\ldots,M). \tag{1.7}$$

In addition, we have the equilibrium relation that correlates n_i as a continuous function of the set $\{c_i\}$ with as many derivatives as may be required:

$$n_i=n_i(c_1,c_2,\ldots,c_M) \quad (i=1,2,\ldots,M). \tag{1.8}$$

Equations (1.7) and (1.8) represent a quasilinear system of M partial differential equations of first order. It has been shown that the solution to Riemann's problem for such equations is given by a one-parameter family so that the image in the hodograph space† lies on a single curve, Γ (Rhee *et al.* 1970). Introducing the differentiation along the curve Γ

$$\frac{\mathscr{D}n_i}{\mathscr{D}c_i}=\sum_{j=1}^{M}\frac{\partial n_i}{\partial c_j}\left(\frac{\mathrm{d}c_j}{\mathrm{d}c_i}\right)_{\Gamma}, \tag{1.9}$$

we can deduce from equation (1.7) the equation

$$\sigma=\left(\frac{\mathrm{d}\tau}{\mathrm{d}x}\right)_{\omega}=\epsilon\frac{1+\nu\mathscr{D}n_i/\mathscr{D}c_i}{1-\mu\mathscr{D}n_i/\mathscr{D}c_i}, \tag{1.10}$$

where ω is the parameter running along the curve Γ. Since σ must be independent of the subscript i, we obtain the equation

$$\frac{\mathscr{D}n_1}{\mathscr{D}c_1}=\frac{\mathscr{D}n_2}{\mathscr{D}c_2}=\ldots=\frac{\mathscr{D}n_M}{\mathscr{D}c_M}, \tag{1.11}$$

which is the fundamental differential equation of the present problem.

Rearranging equation (1.10), we obtain

$$\frac{\mathscr{D}n_i}{\mathscr{D}c_i}=\frac{\sigma-\epsilon}{\mu\sigma+\nu\epsilon} \quad (j=1,2,\ldots,M) \tag{1.12}$$

which, upon expansion, can be rewritten in the form

$$\frac{\partial n_i}{\partial c_1}\frac{\mathrm{d}c_1}{\mathrm{d}\omega}+\ldots+\frac{\partial n_i}{\partial c_{i-1}}\frac{\mathrm{d}c_{i-1}}{\mathrm{d}\omega}+\left(\frac{\partial n_i}{\partial c_i}-\frac{\sigma-\epsilon}{\mu\sigma+\nu\epsilon}\right)\frac{\mathrm{d}c_i}{\mathrm{d}\omega}+\frac{\partial n_i}{\partial c_{i+1}}\frac{\mathrm{d}c_{i+1}}{\mathrm{d}\omega}+\ldots+\frac{\partial n_i}{\partial c_M}\frac{\mathrm{d}c_M}{\mathrm{d}\omega}=0 \quad (i=1,2,\ldots,M)$$

or briefly in matrix form

$$\left(\nabla\boldsymbol{n}-\frac{\sigma-\epsilon}{\mu\sigma+\nu\epsilon}\boldsymbol{I}\right)\frac{\mathrm{d}\boldsymbol{c}}{\mathrm{d}\omega}=0, \tag{1.13}$$

where $\mathrm{d}/\mathrm{d}\omega$ represents the differentiation with ω as the independent variable along the Γ. In equation (1.13) ∇ represents the gradient in the hodograph space and $\boldsymbol{n}$ or $\boldsymbol{c}$ denotes the column vector of M elements, $\{n_i\}$ or $\{c_i\}$, respectively. The existence of Γ requires the condition

$$\left|\nabla\boldsymbol{n}-\frac{\sigma-\epsilon}{\mu\sigma+\nu\epsilon}\boldsymbol{I}\right|=0. \tag{1.14}$$

The system (1.7), on the other hand, can be put into matrix form

$$(\boldsymbol{I}-\mu\nabla\boldsymbol{n})\frac{\partial\boldsymbol{c}}{\partial x}+\epsilon(\boldsymbol{I}+\nu\nabla\boldsymbol{n})\frac{\partial\boldsymbol{c}}{\partial\tau}=0, \tag{1.15}$$

† The M-dimensional space of dependent variables will be called the hodograph space.

Downloaded from rsta.royalsocietypublishing.org

and thus the characteristic direction, according to the mathematical theory, is given by the eigenvalue λ of the matrix $\epsilon(\boldsymbol{I}-\mu\nabla\boldsymbol{n})^{-1}(\boldsymbol{I}+\nu\nabla\boldsymbol{n})$ if $(\boldsymbol{I}-\mu\nabla\boldsymbol{n})$ is non-singular. In other words, the characteristic direction λ must satisfy the equation

$$|\epsilon(\boldsymbol{I}-\mu\nabla\boldsymbol{n})^{-1}(\boldsymbol{I}+\nu\nabla\boldsymbol{n})-\lambda\boldsymbol{I}|=0$$

or, by applying the rule for the product of matrices,

$$\left|\nabla\boldsymbol{n}-\frac{\lambda-\epsilon}{\mu\lambda+\nu\epsilon}\boldsymbol{I}\right|=0. \tag{1.16}$$

Comparing equation (1.16) with equation (1.14), we conclude that σ defined by equation (1.10) represents the characteristic direction of the system (1.7).

(*b*) *Discontinuous field*

Suppose the distribution of solutes contains a discontinuity within the domain† of interest. Such a discontinuity is governed by the same principle of conservation of mass, which may be formulated as a balance across the discontinuity and, in terms of the dimensionless variables, gives the equation

$$\sigma^{s}\equiv\left(\frac{\mathrm{d}\tau}{\mathrm{d}x}\right)^{s}=\epsilon\frac{1+\nu[n_i]/[c_i]}{1-\mu[n_i]/[c_i]}. \tag{1.17}$$

Here the bracket [ ] denotes the jump of the quantity enclosed across the discontinuity. Equation (1.17) is the generalized Rankine–Hugoniot relation and σ^{s} represents the reciprocal of the propagation speed of the discontinuity.

Since adsorption equilibrium is established, equation (1.17) holds for every i and therefore we have the compatibility condition

$$\frac{[n_1]}{[c_1]}=\frac{[n_2]}{[c_2]}=\ldots=\frac{[n_M]}{[c_M]} \tag{1.18}$$

which must be satisfied across a discontinuity.

Equations (1.17) and (1.18) form a system of M algebraic equations so that, given the state on one side, the state across the discontinuity can be determined if one of the c_i's or σ^{s} is given. Consequently, the state on the opposite side of a discontinuity is given by a one-parameter family.

The state, however, is not determined uniquely because the ratio $[n_i]/[c_i]$ is independent of the jump direction. In order to select the physically relevant solution, it is necessary to introduce an additional condition that specifies the jump direction appropriately. Such a condition, which is called the entropy condition, can be deduced from the conservation law for the continuous field, more specifically from equation (1.10) (cf. §2(*c*)).

(*c*) *Initial and boundary conditions*

For a Riemann's problem with finite domain we shall have data prescribed as follows:

$$\text{at}\quad \tau=0,\quad c_i=c_i^{\mathrm{i}}\quad \text{for}\quad 0<x<1; \tag{1.19}$$

$$\text{at}\quad x=0,\quad c_i=c_i^{\mathrm{a}}\quad \text{for}\quad \tau>0; \tag{1.20}$$

$$\text{at}\quad x=1,\quad n_i=n_i^{\mathrm{b}}\quad \text{for}\quad \tau>0. \tag{1.21}$$

Since equilibrium may not be established outside the contacting region (domain), the states of the outgoing flows (n_i^{a} and c_i^{b}) cannot be determined, in general, from the above.

† Here the domain coincides with the region of contact between phases; i.e. $0<x<1$ and $\tau>0$.

PHILOSOPHICAL TRANSACTIONS OF THE ROYAL SOCIETY A MATHEMATICAL, PHYSICAL & ENGINEERING SCIENCES

PHILOSOPHICAL TRANSACTIONS OF THE ROYAL SOCIETY A MATHEMATICAL, PHYSICAL & ENGINEERING SCIENCES

Downloaded from rsta.royalsocietypublishing.org

The conservation law, on the other hand, requires that the conditions

$$\frac{1}{\mu} = \frac{n_i^{\mathrm{a}} - n_i^{0+}}{c_i^{\mathrm{a}} - c_i^{0+}} \tag{1.22}$$

$$= \frac{n_i^{\mathrm{b}} - n_i^{1-}}{c_i^{\mathrm{b}} - c_i^{1-}} \tag{1.23}$$

must be satisfied over the corresponding boundary where n_i^{0+} and n_i^{1-} are the equilibrium values corresponding to c_i^{0+} and c_i^{1-}, respectively. These conditions are sufficient to determine the states of the outgoing flows and, in fact, are the relevant boundary conditions. It is interesting to note their analogy to a free boundary condition. Although c_i^{a} and n_i^{b} remain constant, n_i^{a} and c_i^{b} may not be constant.

By applying the conditions (1.22) and (1.23) we allow the appearance of a discontinuity at either boundary. Such a discontinuity will be called the boundary discontinuity and must be distinguished from that discussed in §1 (*b*). In the following we shall denote the boundaries at $x = 0$ and $x = 1$ by the symbols $\mathscr{B}^{\mathrm{a}}$ and $\mathscr{B}^{\mathrm{b}}$, respectively

2. Basic theory

It is remarkable that the fundamental differential equation (1.11) and also the compatability condition (1.18) are independent not only of the system parameter ν but also of the motion of each phase μ. The image of a solution in the hodograph space is therefore invariant under variation of speed of either phase and intrinsic to the equilibrium relationship between phases.

We shall now assume that the equilibrium is represented by the Langmuir adsorption isotherm

$$n_i = \frac{NK_i c_i}{1 + \sum_{j=1}^{M} K_j c_j} \quad (i = 1, 2, \ldots, M), \tag{2.1}$$

in which N is the saturation value of n_i and K_i is the isotherm parameter intrinsic to the solute A_i and the adsorbent. To avoid duplication extensive references will be made to the previous article by Rhee *et al.* (1970).

(*a*) *Riemann invariants and characteristic parameters*

For the Langmuir adsorption isotherm (2.1) we found that the compatibility condition (1.18) is an integral of the fundamental differential equation (1.11), and that there are M different kinds of solution. Of these the kth kind, for example, is given by the one-parameter family

$$\phi_i - \phi_i^{\circ} = J_i^{(k)}(D - D^{\circ}) \quad (i = 1, 2, \ldots, M), \tag{2.2}$$

where

$$\phi_i = K_i c_i, \tag{2.3}$$

$$D = 1 + \sum_{i=1}^{M} K_i c_i, \tag{2.4}$$

and the superscript o denotes a fixed state. Note that the parameter D may be related to the coverage Θ of adsorption sites by the equation

$$\Theta \equiv \sum_{i=1}^{M} n_i / N = 1 - 1/D. \tag{2.5}$$

Equation (2.2) shows that each $I^{(k)}$ is straight and passes through the fixed point $\{\phi_i^{\circ}\}$ in the

Downloaded from rsta.royalsocietypublishing.org

hodograph space $\Phi(M)$. Its direction is given by the kth Riemann invariant $J_i^{(k)}$, which remains constant along the $\Gamma^{(k)}$ and, for the Langmuir isotherm, takes the form

$$J_i^{(k)} = \frac{K_i n_i}{NK_i - \omega_{(k)}}. \tag{2.6}$$

The characteristic parameter $\omega_{(k)}$, given by the kth root of the Mth order algebraic equation

$$\sum_{i=1}^{M} \frac{K_i n_i}{NK_i - \omega} = 1 \tag{2.7}$$

is the only parameter varying along the $\Gamma^{(k)}$. Equation (2.7) is a continuous transformation of the hodograph space $\Phi(M)$ onto the ω-space $\Omega(M)$. Since it is one-to-one and its inverse

$$\phi_i = \left(\frac{NK_i}{\omega_{(i)}} - 1\right) \prod_{\substack{j=1 \\ j \neq i}}^{M} \frac{1 - NK_i/\omega_{(j)}}{1 - K_i/K_j} \quad (i = 1, 2, \ldots, M) \tag{2.8}$$

is also continuous, the transformation defines a homeomorphism between the two spaces and this corresponds to the h-transformation of Hellferich (1968). It is clear from the above that the image of a $\Gamma^{(k)}$ in $\Omega(M)$ falls on a straight line parallel to the $\omega_{(k)}$-axis.

Another useful form of invariant is

$$\Lambda_{(k)} \equiv NK_i(D - \phi_i/J_i^{(k)}) = \omega_{(k)} D, \tag{2.9}$$

which is independent of the choice of i and remains constant along a $\Gamma^{(k)}$. It follows from equation (2.7) that

$$0 \leqslant \omega_{(1)} < \omega_{(2)} < \ldots < \omega_{(M)} \leqslant NK_M, \tag{2.10}$$

and hence

$$0 \leqslant \Lambda_{(1)} < \Lambda_{(2)} < \ldots < \Lambda_{(M)}. \tag{2.11}$$

(*b*) *Characteristics and simple waves*

Since there are M different kinds of Γ, there correspond M different values of σ:

$$\sigma_{(k)} \equiv \left(\frac{\mathrm{d}\tau}{\mathrm{d}x}\right)_{\omega_{(k)}} = \epsilon \frac{D + \nu\omega_{(k)}}{D - \mu\omega_{(k)}} \tag{2.12}$$

$$= \epsilon \frac{D^2 + \nu\Lambda_{(k)}}{D^2 - \mu\Lambda_{(k)}} \tag{2.13}$$

for $k = 1, 2, \ldots, M$ and accordingly M different kinds of characteristics exist as befits a totally hyperbolic system. It follows from equation (2.10) or (2.11) that

$$\frac{1}{\epsilon} > \frac{1}{\sigma_{(1)}} > \frac{1}{\sigma_{(2)}} > \ldots > \frac{1}{\sigma_{(M)}} > -\frac{\mu}{\epsilon\nu}. \tag{2.14}$$

A $C^{(k)}$ grows steeper as μ increases until it becomes vertical when

$$\mu = \mu^{(k)} \equiv D/\omega_{(k)}. \tag{2.15}$$

We shall call $\mu^{(k)}$ the critical ratio of flow rates for the $C^{(k)}$. For flow rate ratios above the critical value $C^{(k)}$ is directed backwards.

According to the simple wave theory, the (k)-Riemann invariants remain constant in a (k)-simple wave region and thus the region in the physical plane is covered by a family of straight

Downloaded from rsta.royalsocietypublishing.org

(k)-characteristics $C^{(k)}$ which carry constant values of ϕ_i. The image in $\Omega(M)$ falls on a $I^{\gamma(k)}$ and thus the state is represented by a one-parameter family, equation (2.2).

Since it is required of a (k)-simple wave to have

$$\frac{\partial \sigma_{(k)}}{\partial x} = \left(\frac{\partial \sigma_{(k)}}{\partial D}\right)_{\Lambda_{(k)}} \frac{\partial D}{\partial x} < 0,$$

whereas it follows from equation (2.13) that

$$\left(\frac{\partial \sigma_{(k)}}{\partial D}\right)_{\Lambda_{(k)}} < 0$$

for any k, we conclude that in a simple wave D, and thus also the coverage Θ, increase in the x-direction. Note that $\omega_{(k)}$ is inversely proportional to the parameter D in the (k)-simple wave.

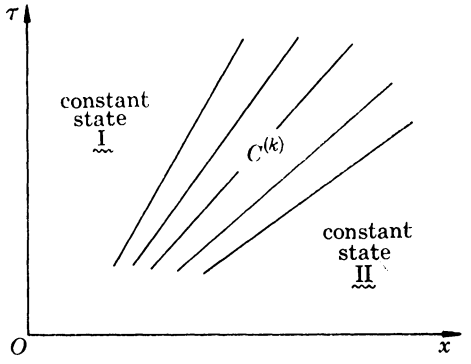

FIGURE 2. Physical plane portrait of a (k)-simple wave. $D^{\mathrm{I}} < D^{\mathrm{II}}$; $\omega^{\mathrm{I}}_{(k)} > \omega^{\mathrm{II}}_{(k)}$; $\Lambda_{(k)} = \text{constant}$.

For a (k)-simple wave it seems appropriate to define two critical values of μ; one is the lower critical ratio (cf. figure 2 for notation)

$$\mu^{(k)}_{*} \equiv D^{\mathrm{I}}/\omega^{\mathrm{I}}_{(k)} \tag{2.16}$$

and the other is the upper critical ratio

$$\mu^{*(k)} \equiv D^{\mathrm{II}}/\omega^{\mathrm{II}}_{(k)}. \tag{2.17}$$

It then follows that for $\mu < \mu^{(k)}_{*}$ the (k)-simple wave is forward-facing and for $\mu > \mu^{*(k)}$ it is backward-facing, whereas for $\mu^{(k)}_{*} \leqslant \mu \leqslant \mu^{*(k)}$ there exists a vertical $C^{(k)}$ so that the corresponding state is stationary.

It can be shown from equation (2.13) that

$$\left.\begin{aligned} \frac{\partial}{\partial D}\left(\frac{\partial \sigma_{(k)}}{\partial \mu}\right) \quad & < 0 \quad \text{if} \quad \sigma_{(k)} > 0, \\ & > 0 \quad \text{if} \quad \sigma_{(k)} < 0. \end{aligned}\right\} \tag{2.18}$$

As μ increases, therefore, a (k)-simple wave becomes more expansive if it is forward-facing and becomes less expansive if it is backward-facing.

(c) *Shock waves*

If the parameter D decreases in the x-direction, a physically impossible situation with overlapping characteristics obtains, and the state cannot be described by a continuous solution. Consequently, a discontinuous solution must be introduced which will be governed by the entropy

Downloaded from rsta.royalsocietypublishing.org

condition, namely that at a point of discontinuity the parameter D and so the coverage Θ decrease from the left-hand side to the right.

Since the compatibility condition is an integral of the fundamental differential equation, it is clear that there are M different kinds of discontinuity. The image of a discontinuity in $\Omega(M)$, if it is of the kth kind, falls on a $\Gamma^{(k)}$. A discontinuity of the kth kind, therefore, connects the states on both sides by a one-parameter family

$$[\phi_i] = J_i^{(k)}[D] \quad (i = 1, 2, \ldots, M) \tag{2.19}$$

and propagates in the direction

$$\sigma^{\mathrm{s}}_{(k)} \equiv \left(\frac{\mathrm{d}\tau}{\mathrm{d}x}\right)^{\mathrm{s}}_{(k)} = \epsilon \frac{D^{\mathrm{l}} D^{\mathrm{r}} + \nu \Lambda_{(k)}}{D^{\mathrm{l}} D^{\mathrm{r}} - \mu \Lambda_{(k)}}. \tag{2.20}$$

where the superscripts l and r denote the left- and right-hand sides of the discontinuity, respectively. Here the invariant $\Lambda_{(k)}$ is given by

$$\Lambda_{(k)} \equiv \omega^{\mathrm{l}}_{(k)} D^{\mathrm{l}} = \omega^{\mathrm{r}}_{(k)} D^{\mathrm{r}}. \tag{2.21}$$

Consequently, equation (2.20) can be rewritten in the form

$$\sigma^{\mathrm{s}}_{(k)} = \epsilon \frac{D^{\mathrm{l}} + \nu \omega^{\mathrm{r}}_{(k)}}{D^{\mathrm{l}} - \mu \omega^{\mathrm{r}}_{(k)}} \tag{2.22}$$

$$= \epsilon \frac{D^{\mathrm{r}} + \nu \omega^{\mathrm{l}}_{(k)}}{D^{\mathrm{r}} - \mu \omega^{\mathrm{l}}_{(k)}}. \tag{2.23}$$

It then follows from the inequality (2.10) that, with a fixed state on one side,

$$\frac{1}{\epsilon} > \frac{1}{\sigma^{\mathrm{s}}_{(1)}} > \frac{1}{\sigma^{\mathrm{s}}_{(2)}} > \ldots > \frac{1}{\sigma^{\mathrm{s}}_{(M)}} > -\frac{\mu}{\epsilon\nu}. \tag{2.24}$$

On the other hand, by comparing equations (2.22) and (2.23) with equation (2.12) and using the entropy condition we can show that

$$\frac{1}{\sigma^{\mathrm{l}}_{(k)}} > \frac{1}{\sigma^{\mathrm{s}}_{(k)}} > \frac{1}{\sigma^{\mathrm{r}}_{(k)}} \tag{2.25}$$

and further, by introducing equation (2.10), we obtain the inequality

$$\frac{1}{\sigma^{\mathrm{l}}_{(k+1)}} < \frac{1}{\sigma^{\mathrm{s}}_{(k)}} < \frac{1}{\sigma^{\mathrm{r}}_{(k-1)}}. \tag{2.26}$$

According to Lax (1957), equations (2.25) and (2.26) are precisely the inequalities characterizing shocks. An immediate consequence is that every discontinuity appearing in the domain is a shock.

A (k)-shock line $S^{(k)}$ grows steeper as μ increases and becomes vertical when

$$\mu = \mu^{\mathrm{s}(k)} \equiv D^{\mathrm{l}}/\omega^{\mathrm{r}}_{(k)} = D^{\mathrm{r}}/\omega^{\mathrm{l}}_{(k)}. \tag{2.27}$$

For this critical ratio $\mu^{\mathrm{s}(k)}$ the (k)-shock becomes stationary and for $\mu > \mu^{\mathrm{s}(k)}$ the shock propagates backwards.

We notice that, for the fluid phase,

$$\frac{\mathrm{d}x}{\mathrm{d}\tau} = \frac{1}{\epsilon} \tag{2.28}$$

and, for the solid phase,

$$\frac{\mathrm{d}x}{\mathrm{d}\tau} = -\frac{v}{\epsilon u}. \tag{2.29}$$

Comparing these with equation (2.24), we find that no shock can propagate faster than the fluid phase when moving forwards or than the solid phase when going backwards. The same is true

Downloaded from rsta.royalsocietypublishing.org

for any disturbance that is represented by a discontinuity in some derivatives since it propagates along the characteristics (cf. equation (2.14)).

It can be shown that entropy increases across a shock from the right-hand side to the left; i.e. in the direction of increasing coverage Θ. This remarkable observation proves that the entropy condition is consistent with the second law of thermodynamics. Details will be presented in a forthcoming monograph.

(*d*) *Patterns of interaction*

Since every wave can face either forward or backward depending upon the parameter μ, it is to be expected that two adjacent waves may meet in the domain and influence each other. Such a phenomenon is called an interaction.

The inequalities (2.14), (2.24), (2.25) and (2.26) specify the sets of waves that can interact (Patterns of interaction) and the image in the space $\Omega(M)$ illuminates the mechanism of each pattern (Basic principles of interaction). Since both the patterns and principles of interaction are independent of μ, it is clear that they remain the same as those that have been established for the fixed bed chromatography (cf. Rhee *et al.* 1970). There are only three different patterns with different principles and we shall briefly rephrase these as follows:

Pattern I (*superposition*). Two shock waves of the same kind necessarily interact with each other and are superposed instantly.

Pattern II (*absorption*). A simple wave necessarily interacts with a shock wave of the same kind and is absorbed by the latter.

Pattern III (*transmission*). A (k)-wave necessarily interacts with an (m)-wave, travelling ahead of it if $m > k$, or travelling behind it if $m < k$, and is transmitted across it.

In the region of interaction the state varies along each characteristic or on one or both sides of the shock involved and thus the wave propagation gets accelerated or decelerated. When a (k)-simple wave is transmitted across an (m)-wave where $m \neq k$, the parameter $\omega_{(k)}$ remains invariant along each $C^{(k)}$. In addition, it follows from equation (2.12) that

$$\left(\frac{\partial \sigma_{(k)}}{\partial D}\right)_{\omega_{(k)}} < 0.$$

An immediate consequence is that, if D increases along a $C^{(k)}$, the disturbance carried by it is accelerated or vice versa.

When a (k)-shock is superposed or absorbed by another (k)-wave, the invariant $\Lambda_{(k)}$ remains constant throughout. On the other hand, if a (k)-shock is transmitted across an (m)-wave where $m \neq k$, the parameter $\omega_{(k)}$ remains constant on both sides. It can be shown directly from equations (2.20), (2.22) and (2.23) that

$$\left(\frac{\partial \sigma^{\mathrm{s}}_{(k)}}{\partial D^{\mathrm{r}}}\right)_{\Lambda_{(k)}} < 0, \quad \left(\frac{\partial \sigma^{\mathrm{s}}_{(k)}}{\partial D^{\mathrm{l}}}\right)_{\Lambda_{(k)}} < 0;$$

$$\left(\frac{\partial \sigma^{\mathrm{s}}_{(k)}}{\partial D^{\mathrm{r}}}\right)_{\omega^{\mathrm{l}}_{(k)}} < 0, \quad \left(\frac{\partial \sigma^{\mathrm{s}}_{(k)}}{\partial D^{\mathrm{l}}}\right)_{\omega^{\mathrm{r}}_{(k)}} < 0;$$

and hence a shock is accelerated if D^{r} and/or D^{l} increase as it propagates or vice versa.

PHILOSOPHICAL TRANSACTIONS OF THE ROYAL SOCIETY A MATHEMATICAL, PHYSICAL & ENGINEERING SCIENCES

PHILOSOPHICAL TRANSACTIONS OF THE ROYAL SOCIETY A MATHEMATICAL, PHYSICAL & ENGINEERING SCIENCES

Downloaded from rsta.royalsocietypublishing.org

3. Semi-infinite column

In this section we shall assume that the contacting region extends indefinitely beyond the point $x = 1$ and the data are specified as

$$\left.\begin{aligned} &\text{at} \quad \tau = 0, \quad \phi_m = \phi_m^{\mathrm{i}} \quad \text{for} \quad x > 0; \\ &\text{at} \quad x = 0, \quad \phi_m = \phi_m^{\mathrm{a}} \quad \text{for} \quad \tau > 0; \end{aligned}\right\} \tag{3.1}$$

for $m = 1, 2, \ldots, M$. This is a Riemann's problem.

For $\mu = 0$ (fixed bed) the solution has been given previously in terms of constant states separated by centred simple and shock waves (Rhee *et al.* 1970). The M waves are ordered counterclockwise from the (1)-wave to the (M)-wave and the (k)-constant state $\{\phi_m^{(k)}\}$ that appears between the (k)- and $(k+1)$-waves is given by the equations

$$D^{(k)} = D^{\mathrm{i}} \prod_{j=1}^{k} \frac{\omega_{(j)}^{\mathrm{i}}}{\omega_{(j)}^{\mathrm{a}}} = D^{\mathrm{a}} \prod_{j=k+1}^{M} \frac{\omega_{(j)}^{\mathrm{a}}}{\omega_{(j)}^{\mathrm{i}}} \tag{3.2}$$

and

$$\phi_m^{(k)} = \phi_m^{\mathrm{i}} \prod_{j=1}^{k} \frac{1 - NK_m/\omega_{(j)}^{\mathrm{a}}}{1 - NK_m/\omega_{(j)}^{\mathrm{i}}} = \phi_m^{\mathrm{a}} \prod_{j=k+1}^{M} \frac{1 - NK_m/\omega_{(j)}^{\mathrm{i}}}{1 - NK_m/\omega_{(j)}^{\mathrm{a}}}, \tag{3.3}$$

where the sets $\{\omega_{(j)}^{\mathrm{i}}\}$ and $\{\omega_{(j)}^{\mathrm{a}}\}$ represent the images of the initial and entry data in $\Omega(M)$, respectively. Construction of wave solutions in the physical plane is straightforward, and the criterion concerning the wave type is given as follows: the (k)-wave is a simple wave if $\omega_{(k)}^{\mathrm{i}} < \omega_{(k)}^{\mathrm{a}}$ and it is a shock wave if $\omega_{(k)}^{\mathrm{i}} > \omega_{(k)}^{\mathrm{a}}$. The regions of M waves so constructed and $M-1$ constant states in between represent the range of influence of the discontinuity at the origin.

The image of the solution in $\Omega(M)$ is independent of μ and so are equations (3.2) and (3.3). The criterion concerning wave type (entropy condition) is also independent of μ. For sufficiently small values of μ, therefore, the solution can be determined by applying, in principle, the same procedure as for fixed bed problems.

Here we notice that, as μ increases, the range of influences rotates counterclockwise maintaining its overall feature because every characteristic as well as shock line becomes steeper. It is then expected that for certain values of μ one part of the range of influence lies in the domain while the other part lies outside. Along the line $x = 0+$ there corresponds a unique state $\{\phi_m^{0+}\}$. This implies that the discontinuity at the origin is split into two parts $\{\phi_m^{\mathrm{i}} - \phi_m^{0+}\}$ and $\{\phi_m^{0+} - \phi_m^{\mathrm{a}}\}$. The first part influences the solution in the domain in such a way that equation (1.7) is satisfied, whereas the second part influences the state of the outgoing solid phase in such a way that equation (1.22) is satisfied. Application of equation (1.22) is straightforward since each of the M equations is independent. This will result in a boundary discontinuity on $\mathscr{B}^{\mathrm{a}}$.

The remaining question now is how to determine the state $\{\phi_m^{0+}\}$ for a given value of μ. Various situations are expected to arise over the whole spectrum of μ but those can be classified appropriately into four categories by making cuts at every critical value along the μ-spectrum. Here the critical values are given as follows:

If $\omega_{(k)}^{\mathrm{a}} > \omega_{(k)}^{\mathrm{i}}$,

$$\left.\begin{aligned} \mu_*^{(k)} &= D^{(k)}/\omega_{(k)}^{\mathrm{a}}, \\ \mu^{*(k)} &= D^{(k-1)}/\omega_{(k)}^{\mathrm{i}}, \end{aligned}\right\} \tag{3.4}$$

and if $\omega_{(k)}^{\mathrm{a}} < \omega_{(k)}^{\mathrm{i}}$,

$$\mu_*^{(k)} = \mu^{*(k)} = \mu^{s(k)} = D^{(k)}/\omega_{(k)}^{\mathrm{i}} \tag{3.5}$$

for $k = 1, 2, \ldots, M$ with $D^{(M)} \equiv D^{\mathrm{a}}$ and $D^{(0)} \equiv D^{\mathrm{i}}$.

PHILOSOPHICAL TRANSACTIONS OF THE ROYAL SOCIETY A MATHEMATICAL, PHYSICAL & ENGINEERING SCIENCES
PHILOSOPHICAL TRANSACTIONS OF THE ROYAL SOCIETY A MATHEMATICAL, PHYSICAL & ENGINEERING SCIENCES

Downloaded from rsta.royalsocietypublishing.org

(i) *Lower range*

This range corresponds to the portion

$$0 \leqslant \mu < \mu_*^{(M)} \tag{3.6}$$

of the μ-spectrum. The whole range of influence lies in the domain and thus $\phi_m^{0+} = \phi_m^{\mathrm{a}}$. Equation (1.22) then becomes trivial and simply yields $n_m^{\mathrm{a}} = n_{m,\mathrm{eq}}^{\mathrm{a}}$ where $n_{m,\mathrm{eq}}^{\mathrm{a}}$ represents the equilibrium value corresponding to the state $\{\phi_m^{\mathrm{a}}\}$. The solution is continuous across the boundary and equilibrium is established at the boundary $\mathscr{B}^{\mathrm{a}}$.

A schematic diagram of the solution is shown in figure 3 (*a*). The boundary $\mathscr{B}^{\mathrm{a}}$ is inward space-like (cf. Courant & Friedrichs 1948). In view of the way in which its data is transmitted such a boundary will be called an emissive boundary.

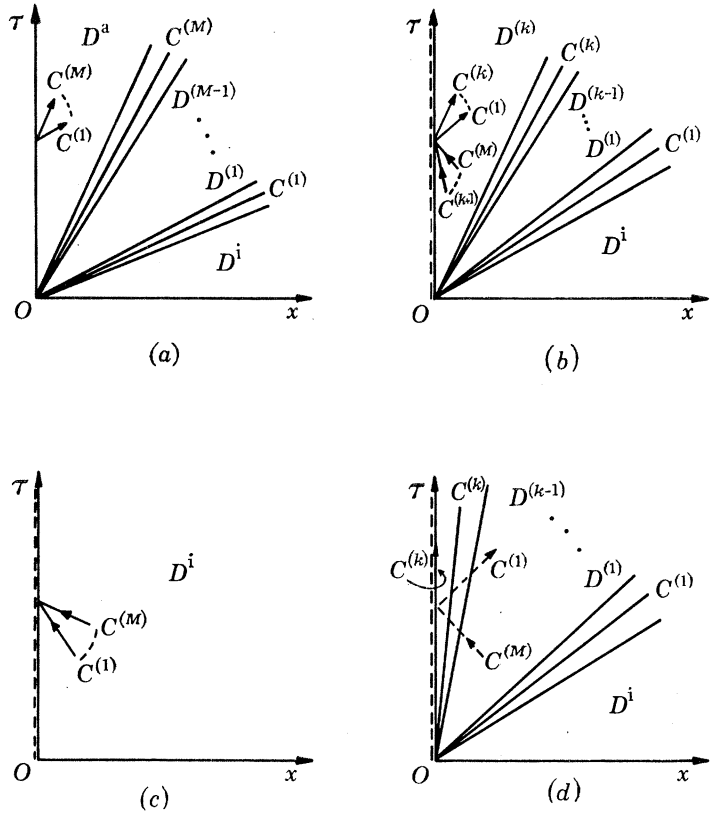

FIGURE 3. Schematic portrait of solutions in the physical plane for various ranges of μ (semi-infinite column). (*a*) Lower range; (*b*) (k)-intermediate range; (*c*) upper range; (*d*) (k)-transition range. ⋯⋯, Boundary discontinuity.

(ii) (k)-*intermediate range*

Along the μ-spectrum this range covers the portion

$$\mu^{*(k+1)} < \mu < \mu_*^{(k)}. \tag{3.7}$$

Only the first k waves are directed forward and $\phi_m^{0+} = \phi_m^{(k)}$. The solution is discontinuous across the boundary and the state $\{n_m^{\mathrm{a}}\}$ is not given by the equilibrium relation but by equation (1.22).

Figure 3 (*b*) illustrates the physical plane portrait of a solution. The boundary $\mathscr{B}^{\mathrm{a}}$ is time-like with the first k characteristics ($C^{(1)} \sim C^{(k)}$) directed forward and the next $M-k$ ones ($C^{(k+1)} \sim C^{(M)}$)

Downloaded from rsta.royalsocietypublishing.org

backward. One may regard the characteristics to be reflected at a time-like boundary as shown in figure 3(*b*) (cf. the characteristics of the linear wave equation). A time-like boundary is partially emissive and partially absorptive in the data transmitting behaviour.

(iii) *Upper range*

Here the parameter μ has the range

$$\mu^{*(1)} < \mu < \infty. \tag{3.8}$$

The range of influence completely falls outside the domain and this implies that the entry data $\{\phi^{\mathrm{a}}_m\}$ have no influence on the solution in the domain so that $\phi^{0+}_m = \phi^{\mathrm{i}}_m$. The entry data, however, determines the state $\{n^{\mathrm{a}}_m\}$ through the boundary discontinuity $\{\phi^{\mathrm{i}}_m - \phi^{\mathrm{a}}_m\}$ on $\mathscr{B}^{\mathrm{a}}$.

In figure 3(*c*) it is shown that the boundary $\mathscr{B}^{\mathrm{a}}$ is outward space-like and therefore absorptive.

(iv) (k)-*transition range*

This corresponds to the portion between the lower and upper critical ratios for the (k)-wave:

$$\mu^{(k)}_* \leqslant \mu \leqslant \mu^{*(k)}. \tag{3.9}$$

In the case of a (k)-simple wave, the region is cut by the τ-axis on the left-hand side and to the given value of μ there corresponds a vertical $C^{(k)}$ which coincides with the τ-axis. The state $\{\phi^{0+}_m\}$ along this $C^{(k)}$ is stationary at $x = 0+$ and determined by the equations

$$D^{0+} = (\mu\omega^{\mathrm{a}}_{(k)} D^{(k)})^{\frac{1}{2}} \tag{3.10}$$

and

$$\phi^{0+}_m = \phi^{(k)}_m + J^{(k)}_m (D^{0+} - D^{(k)}). \tag{3.11}$$

Outside the domain there appears a boundary discontinuity $\{\phi^{0+}_m - \phi^{\mathrm{a}}_m\}$ characterized by equation (1.22). The boundary $\mathscr{B}^{\mathrm{a}}$ is (k)-characteristic and has the nature of a partially emissive and partially absorptive boundary (see figure 3(*d*)).

If the (k)-wave is a shock, this range degenerates to a single point $D^{(k)}/\omega^{\mathrm{i}}_{(k)}$ for which the (k)-shock becomes stationary at $x = 0$ and coalesces with the boundary discontinuity. Hence, the situation will be the same as for the $(k-1)$-intermediate range. The case of $k = M$ is exceptional because the discontinuity on $\mathscr{B}^{\mathrm{a}}$ is not a boundary one but an (M)-shock so that equilibrium is established across it.

In summary, the μ-spectrum consists of one lower range, one upper range, $M-1$ intermediate ranges and M transition ranges. The state of the outgoing solid phase shows a piecewise continuous variation with respect to the parameter μ.

Analogous discussions can be established when the discontinuity is initially imposed at $x = 1$ and the contacting region extends from $x = 1$ to $x = -\infty$, i.e.

$$\left.\begin{aligned} &\text{at} \quad \tau = 0, \quad \phi_m = \phi^{\mathrm{i}}_m \quad \text{for} \quad -\infty < x < 1; \\ &\text{at} \quad x = 1, \quad n_m = n^{\mathrm{b}}_m \quad \text{for} \quad \tau > 0. \end{aligned}\right\} \tag{3.12}$$

Here the sets $\{\omega^{\mathrm{i}}_{(k)}\}$ and $\{\omega^{\mathrm{b}}_{(k)}\}$ takes the roles of $\{\omega^{\mathrm{a}}_{(k)}\}$ and $\{\omega^{\mathrm{i}}_{(k)}\}$ in the previous case, respectively. In the lower range the boundary $\mathscr{B}^{\mathrm{b}}$ becomes outward space-like and thus absorptive. The boundary discontinuity is characterized by equation (1.23). In the upper range the boundary $\mathscr{B}^{\mathrm{b}}$ is inward space-like and emissive. The intermediate and transition ranges can be discussed similarly. The prime interest is, of course, how to determine the state $\{\phi^{1-}_m\}$ and thereby the state $\{\phi^{\mathrm{b}}_m\}$ of the outgoing fluid phase.

PHILOSOPHICAL TRANSACTIONS OF THE ROYAL SOCIETY A MATHEMATICAL, PHYSICAL & ENGINEERING SCIENCES

PHILOSOPHICAL TRANSACTIONS OF THE ROYAL SOCIETY A MATHEMATICAL, PHYSICAL & ENGINEERING SCIENCES

Downloaded from rsta.royalsocietypublishing.org

4. Finite column

In the practice of countercurrent contact, the contacting region is of finite length and the data are prescribed in the form of equations (1.19), (1.20) and (1.21). Basic features of the analysis are expected to remain the same except for the typical nature of the boundaries, $\mathscr{B}^{\mathrm{a}}$ and $\mathscr{B}^{\mathrm{b}}$, that depends upon the parameter μ. In this section, therefore, we shall study mainly the nature of both boundaries over the whole spectrum of μ.

Suppose at the moment that the contacting region extends in both directions so that equilibrium is established everywhere. The images of the initial and entry data in the space $\Omega(M)$ then fall on three different points which will be denoted by I^{i}: $\{\omega^{\mathrm{i}}_{(k)}\}$, E^{a}: $\{\omega^{\mathrm{a}}_{(k)}\}$, and E^{b}: $\{\omega^{\mathrm{b}}_{(k)}\}$, respectively. The image of the solution consists of M segments of distinct $\Gamma^{(k)}$'s arranged in the order of decreasing (k) from E^{a} to I^{i} and another M segments of distinct $\Gamma^{(k)}$'s arranged also in the order of decreasing (k) from I^{i} to E^{b}. In the physical plane, the solution can be determined by combining the two separate solutions discussed in the previous section. After a finite period of time, however, interactions will take place between waves emanating from different points. When every transmissive interaction is over, the image in $\Omega(M)$ is given by M segments of distinct $\Gamma^{(k)}$'s arranged in the order of decreasing (k) from E^{a} directly to E^{b}. Consequently, the (k)-constant state $\{\phi^{(k)}_m\}$ is determined by the equations

$$D^{(k)} = D^{\mathrm{a}} \prod_{j=k+1}^{M} \frac{\omega^{\mathrm{a}}_{(j)}}{\omega^{\mathrm{b}}_{(j)}} = D^{\mathrm{b}}_{\mathrm{eq}} \prod_{j=1}^{k} \frac{\omega^{\mathrm{b}}_{(j)}}{\omega^{\mathrm{a}}_{(j)}} \tag{4.1}$$

and

$$\phi^{(k)}_m = \phi^{\mathrm{a}}_m \prod_{j=k+1}^{M} \frac{1 - NK_m/\omega^{\mathrm{b}}_{(j)}}{1 - NK_m/\omega^{\mathrm{a}}_{(j)}} = \phi^{\mathrm{b}}_{m,\mathrm{eq}} \prod_{j=1}^{k} \frac{1 - NK_m/\omega^{\mathrm{a}}_{(j)}}{1 - NK_m/\omega^{\mathrm{b}}_{(j)}}, \tag{4.2}$$

where

$$D^{\mathrm{b}}_{\mathrm{eq}} = \left(1 - \sum_{i=1}^{M} n^{\mathrm{b}}_i/N\right)^{-1} \tag{4.3}$$

and

$$\phi^{\mathrm{b}}_{m,\mathrm{eq}} = D^{\mathrm{b}}_{\mathrm{eq}} n^{\mathrm{b}}_m/N. \tag{4.4}$$

We notice that equations (4.1) and (4.2) are independent of μ.

For a finite column, the waves emanating from the origin are forward-facing and those centred at the point, $x = 1$ and $\tau = 0$, are backward-facing. According to pattern III of interaction, with k waves centred at the origin only the next $M-k$ waves can emanate from the other end. (If one or both of (k)-waves are shocks, then the (k)-wave may also emanate from the other end.) It is then obvious that every forward (or backward)-facing wave, after $M-k$ (or k) times of transmissive interaction reaches the other end and encounters there a boundary discontinuity characterized by equation (1.23) (or (1.22)). When the tail of the most slowly propagating wave reaches the opposite end, the steady state is attained since no further change will be observed afterwards. The steady state is, of course, given by the (k)-constant state $\{\phi^{(k)}_m\}$ in the domain and by equations (1.22) and (1.23) outside the domain.

The situation changes over the whole spectrum of μ and an appropriate classification can be achieved by making cuts at critical values of μ defined as follows:

If $\omega^{\mathrm{a}}_{(k)} > \omega^{\mathrm{b}}_{(k)}$,

$$\left.\begin{aligned} \mu^{(k)}_* &= D^{(k)}/\omega^{\mathrm{a}}_{(k)} \\ \mu^{*(k)} &= D^{(k-1)}/\omega^{\mathrm{b}}_{(k)} \end{aligned}\right\} \tag{4.5}$$

and if $\omega^{\mathrm{a}}_{(k)} < \omega^{\mathrm{b}}_{(k)}$,

$$\mu^{(k)}_* = \mu^{*(k)} = \mu^{\mathrm{s}(k)} = D^{(k)}/\omega^{\mathrm{b}}_{(k)} \tag{4.6}$$

for $k = 1, 2, \ldots, M$ with $D^{(M)} \equiv D^{\mathrm{a}}$ and $D^{(0)} \equiv D^{\mathrm{b}}_{\mathrm{eq}}$.

Downloaded from rsta.royalsocietypublishing.org

(i) *Lower range*: $0 \leqslant \mu < \mu_*^{(M)}$

All the waves are forward-facing and the boundary $\mathscr{B}^{\mathrm{a}}$ is inward spacelike while $\mathscr{B}^{\mathrm{b}}$ is outward spacelike. Hence, $\phi_m^{0+} = \phi_m^{\mathrm{a}}$ and $n_m^{\mathrm{a}} = n_{m,\mathrm{eq}}^{\mathrm{a}}$. The entry data at $\mathscr{B}^{\mathrm{b}}$ has no influence on the state in the domain since the domain of dependence never contains $\mathscr{B}^{\mathrm{b}}$ but it determines the state $\{\phi_m^{\mathrm{b}}\}$ which is connected to the state inside by a boundary discontinuity. By applying equation (1.23) we find that ϕ_m^{b} varies from

$$\phi_m^{\mathrm{i}} + \mu K_m (n_m^{\mathrm{b}} - n_m^{\mathrm{i}}) \quad \text{at} \quad \tau = 0+ \qquad \text{to} \qquad \phi_m^{\mathrm{a}} + \mu K_m (n_m^{\mathrm{b}} - n_{m,\mathrm{eq}}^{\mathrm{a}}) \quad \text{at} \quad \tau = \tau_{\mathrm{s.s.}}$$

as shown in figure 4 (*a*).

At $\tau = \tau_{\mathrm{s.s.}}$ the steady state is attained and it is clear that the steady state is given by

$$\left.\begin{aligned} n_m^{\mathrm{a}} &= n_{m,\mathrm{eq}}^{\mathrm{a}} = N\phi_m^{\mathrm{a}}/D^{\mathrm{a}}; \\ \phi_m &= \phi_m^{\mathrm{a}} \quad \text{for} \quad 0 < x < 1; \\ \phi_m^{\mathrm{b}} &= \phi_m^{\mathrm{a}} + \mu K_m (n_m^{\mathrm{b}} - n_{m,\mathrm{eq}}^{\mathrm{a}}). \end{aligned}\right\} \tag{4.7}$$

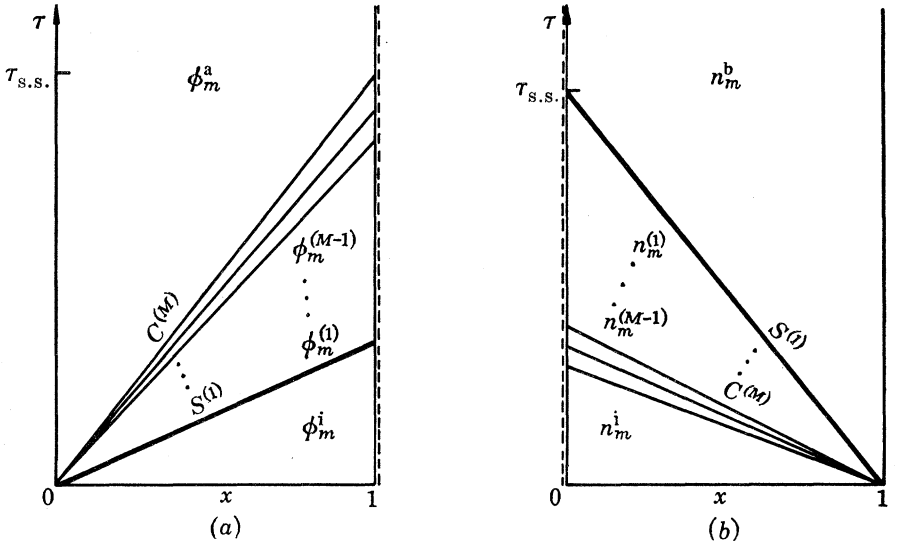

FIGURE 4. Schematic portrait of solutions in the physical plane (finite column). (*a*) For the lower range and (*b*) for the upper range of μ. ·····, Boundary discontinuity.

(ii) *Upper range*: $\mu^{*(1)} < \mu < \infty$

Here all the waves are directed backward and the boundary $\mathscr{B}^{\mathrm{a}}$ is outward spacelike while $\mathscr{B}^{\mathrm{b}}$ is inward spacelike, as shown in figure 4 (*b*). The situations at boundaries are reversed from those for the lower range so that $n_m^{1-} = n_m^{\mathrm{b}}$ and $\phi_m^{\mathrm{b}} = \phi_{m,\mathrm{eq}}^{\mathrm{b}}$, where $\phi_{m,\mathrm{eq}}^{\mathrm{b}}$ represents the equilibrium value corresponding to the state $\{n_m^{\mathrm{b}}\}$ (cf. equation (4.4)). As shown in figure 4 (*b*), n_m^{0+} varies from n_m^{i} to n_m^{b} and accordingly n_m^{a} varies from $n_m^{\mathrm{i}} + (\phi_m^{\mathrm{a}} - \phi_m^{\mathrm{i}})/\mu K_m$ to $n_m^{\mathrm{b}} + (\phi_m^{\mathrm{a}} - \phi_{m,\mathrm{eq}}^{\mathrm{b}})/\mu K_m$.

The steady state is attained at $\tau = \tau_{\mathrm{s.s.}}$ and it is given by

$$\left.\begin{aligned} n_m^{\mathrm{a}} &= n_m^{\mathrm{b}} + (\phi_m^{\mathrm{a}} - \phi_{m,\mathrm{eq}}^{\mathrm{b}})/\mu K_m; \\ \phi_m &= \phi_{m,\mathrm{eq}}^{\mathrm{b}} \quad \text{for} \quad 0 < x < 1; \\ \phi_m^{\mathrm{b}} &= \phi_{m,\mathrm{eq}}^{\mathrm{b}}. \end{aligned}\right\} \tag{4.8}$$

Downloaded from rsta.royalsocietypublishing.org

(iii) (k)-*intermediate range*: $\mu^{*(k+1)} < \mu < \mu_*^{(k)}$

The first k waves are forward-facing and the next $M-k$ waves backward-facing. Both boundaries are timelike and maintain boundary discontinuities. After every transmissive interaction is over, the domain of dependence consists of segments of $\mathscr{B}^{\mathrm{a}}$ and $\mathscr{B}^{\mathrm{b}}$ excluding the initial line $\tau = 0$ so that the state there is determined by the entry data alone and independent of the initial data.

A schematic portrait in the physical plane is shown in figure 5 (a). At $\tau = \tau_{\mathrm{s.s.}}$ when the (k)-wave reaches $\mathscr{B}^{\mathrm{b}}$ and the $(k+1)$-wave $\mathscr{B}^{\mathrm{a}}$, respectively, the steady state is attained and it is clear that we have

$$\left.\begin{aligned} n_m^{\mathrm{a}} &= n_m^{(k)} + (\phi_m^{\mathrm{a}} - \phi_m^{(k)})/\mu K_m; \\ \phi_m &= \phi_m^{(k)} \quad \text{for} \quad 0 < x < 1; \\ \phi_m^{\mathrm{b}} &= \phi_m^{(k)} + \mu K_m (n_m^{\mathrm{b}} - n_m^{(k)}) \end{aligned}\right\} \tag{4.9}$$

at the steady state.

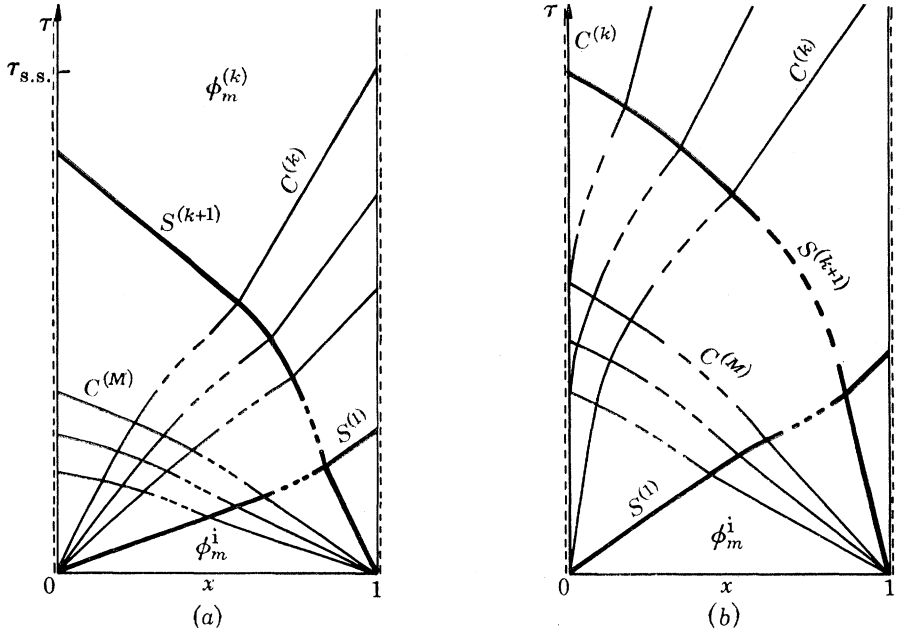

FIGURE 5. Schematic portrait of solutions in the physical plane (finite column). (a) For the (k)-intermediate range and (b) for the (k)-transition range of μ. ⋯⋯, Boundary discontinuity.

(iv) (k)-*transition range*: $\mu_*^{(k)} \leqslant \mu \leqslant \mu^{*(k)}$

If $\omega_{(k)}^{\mathrm{a}} > \omega_{(k)}^{\mathrm{b}}$, one of the boundaries, say $\mathscr{B}^{\mathrm{a}}$, becomes (k)-characteristic so that the corresponding state ϕ_m^{0+} becomes stationary. As shown in figure 5 (b), the first $k-1$ waves are directed forward and the last $M-k$ waves backward while the (k)-wave is cut by $\mathscr{B}^{\mathrm{a}}$. The ultimate value of ϕ_m^{0+} is given by

$$\phi_m^{0+} = \phi_m^{(k)} + J_m^{(k)}(D^{0+} - D^{(k)}) \tag{4.10}$$

in which

$$D^{0+} = (\mu\omega_{(k)}^{\mathrm{a}} D^{(k)})^{\frac{1}{2}} = (\mu\omega_{(k)}^{\mathrm{b}} D^{(k-1)})^{\frac{1}{2}}. \tag{4.11}$$

Both boundaries maintain boundary discontinuities and the steady state is not attained at finite time.

If $\omega_{(k)}^{\mathrm{a}} < \omega_{(k)}^{\mathrm{b}}$, this range degenerates to a single value $D^{(k)}/\omega_{(k)}^{\mathrm{b}}$. In the case when $\omega_{(k)}^{\mathrm{a}} < \omega_{(k)}^{\mathrm{i}} < \omega_{(k)}^{\mathrm{b}}$, two (k)-shocks meet each other in the domain and the superposed (k)-shock becomes stationary. Otherwise, the (k)-shock propagates toward a boundary and coalesces with the boundary

Downloaded from rsta.royalsocietypublishing.org

discontinuity so that the situation will be the same as for the (k)- or $(k-1)$-intermediate range. In both cases the boundaries are time-like and so discontinuous. With the stationary shock at $x = x^s$ $(0 \leqslant x^s \leqslant 1)$, therefore, we have

$$\left.\begin{aligned} n_m^a &= n_m^{(k)} + (\phi_m^a - \phi_m^{(k)})/\mu K_m; \\ \phi_m &= \phi_m^{(k)} \quad \text{for} \quad 0 < x < x^s; \\ \phi_m &= \phi_m^{(k-1)} \quad \text{for} \quad x^s < x < 1; \\ \phi_m^b &= \phi_m^{(k-1)} + \mu K_m (n_m^b - n_m^{(k-1)}). \end{aligned}\right\} \tag{4.12}$$

Note that $\phi_m^{(M)} = \phi_m^a$ and $n_m^{(0)} = n_m^b$. This is a special case of the steady state. If $x^s = 0$ or 1, then equation (4.12) is reduced to equation (4.9) for $k-1$ or k, respectively.

In summary, the μ-spectrum consists of one lower range, one upper range, $M-1$ intermediate ranges, and M transition ranges. Within the domain a unique steady state corresponds to each of the upper, lower, and intermediate ranges. Consequently, there exist $M+1$ possible steady states for a given pair of entry data. The set of steady states are completely determined from the entry data alone while the particular one which is attained depends also on μ. On the other hand, the time $\tau_{s.s.}$ to reach a steady state depends upon the initial and entry data, the parameter μ, and the column length.

If $\omega_{(k)}^a = \omega_{(k)}^b$, the (k)-intermediate range as well as the (k)-transition range is not defined and accordingly the number of possible steady states becomes one less.

In practice we may often have the condition $n_m^i = n_m^b$. All the waves are then centred at the origin and forward-facing. Since no interaction is involved, the analysis becomes fairly simple and yet all the arguments used above remain valid. In particular, the time $\tau_{s.s.}$ for μ in the (k)-intermediate range is given directly by the slope of the uppermost $C^{(k)}$ or $S^{(k)}$; i.e. from equations (2.11) and (2.21),

$$\tau_{s.s.} = \epsilon \frac{D^{(k)} + \nu\omega_{(k)}^a}{D^{(k)} - \mu\omega_{(k)}^a} \quad \text{if} \quad \omega_{(k)}^a > \omega_{(k)}^b \tag{4.13}$$

and

$$\tau_{s.s.} = \epsilon \frac{D^{(k)} + \nu\omega_{(k)}^b}{D^{(k)} - \mu\omega_{(k)}^b} \quad \text{if} \quad \omega_{(k)}^a < \omega_{(k)}^b. \tag{4.14}$$

In the following example we shall be concerned with the determination of various ranges and the steady state. Therefore, the initial condition is arbitrary at the moment. Concentrations are expressed in moles per litre and the parameters are given as $\epsilon = 0.4$ and $N = 1.0$. Further informations are tabulated as follows:

	$m = 1$	2	3	remark
K_m	5.0	7.5	10.0	—
c_m^a	0.150	0.060	0.020	$D^a = 2.40$
n_m^b	0.058	0.309	0.271	$\Theta^b = 0.638$
$\omega_{(m)}^a$	2.445	6.667	9.586	—
$\omega_{(m)}^b$	2.797	5.409	8.974	—

Critical values of μ are evaluated by applying equations (4.1) and (4.5) or (4.6) to determine the ranges of μ:

lower range	$0 \leqslant \mu < 0.250$
(3)-transition range	$0.250 \leqslant \mu \leqslant 0.286$
(2)-intermediate range	$0.286 < \mu < 0.385$
(2)-transition range	$0.385 \leqslant \mu \leqslant 0.584$
(1)-intermediate range	$0.584 < \mu < 1.130$
upper range	$1.130 \leqslant \mu < \infty$.

Downloaded from rsta.royalsocietypublishing.org

There are four different steady states attainable within the domain and these are determined by equation (4.2). If, for instance, μ belongs to the (2)-intermediate range, the steady state attainable is the (2)-constant state $\{c_m^{(2)}\}$ and the states of the outgoing phases are given by equation (4.9). The steady state for $\mu = \frac{1}{3}$ is presented in the following:

	$m=1$	2	3	D	Θ
c_m^{a}	0.150	0.060	0.020	2.40	—
c_m					
$(0 < x < 1)$	0.139	0.045	0.053	2.564	—
c_m^{b}	0.068	0.104	0.074	2.860	—
n_m^{a}	0.304	0.177	0.108	—	0.589
n_m					
$(0 < x < 1)$	0.271	0.132	0.207	—	0.610
n_m^{b}	0.058	0.309	0.271	—	0.638

We observe that more strongly adsorbable solutes A_2 and A_3 are desorbed while the least adsorbable solute A_1 is adsorbed most strongly. The solid phase experiences a slight decrease in the coverage. This example shows that one can achieve the displacement of a strongly adsorbable solute by a less adsorbable solute at the cost of a slight decrease in the coverage. For this example such a displacement can be enhanced by using a lower value of μ.

If the initial condition is prescribed as $n_m^{\mathrm{i}} = n_m^{\mathrm{b}}$, then the time $\tau_{\mathrm{s.s.}}$ is given by equation (4.13) with $k = 2$. For $\mu = \frac{1}{3}$, we obtain $\tau_{\mathrm{s.s.}} = 14.70$.

5. Interaction analysis

In the previous section we observed how interactions may take place between waves issuing from different points of discontinuity. Patterns and principles of such interactions are discussed in §2(*d*). This section is concerned with the separate analysis of each interaction. Obviously, it is permissible to employ the same approach here as for fixed bed problems since the image in the space $\Omega(M)$ is independent of μ. Without loss of generality we shall always consider a case that can be encountered in the operation of a finite column if the value of μ belongs to the (k)-intermediate range.

The physical plane portrait will be given for each case with the parameter D and pertinent characteristic parameters denoted for every constant state. The image in $\Omega(M)$ will not be shown and for this the reader is referred to the previous paper (Rhee *et al.* 1970).

(*a*) *Superposition and absorption*

The waves involved are of the same kind and we shall consider the interaction between a pair of (k)-waves. The image in $\Omega(M)$ lies on a single $\Gamma^{(k)}$ and thus $\Lambda_{(k)}$ remains constant throughout. Among the characteristic parameters, $\omega_{(k)}$ is the only variable one and it is inversely proportional to D (cf. equation (2.9)).

When two (k)-shocks meet each other (head-on collision), the two are superposed instantly as shown in figure 6. The superposed shock is of the kth kind and propagates at a speed given by the reciprocal of

$$\sigma_{(k)}^{\mathrm{s}} = \epsilon \frac{D^{(k)} + \nu\omega_{(k)}^{\mathrm{b}}}{D^{(k)} - \mu\omega_{(k)}^{\mathrm{b}}}. \tag{5.1}$$

As an example of absorptive interaction, we shall consider a case when a (k)-shock wave faces a (k)-simple wave on the right-hand side as shown in figure 7. Since the simple wave is absorbed

Downloaded from rsta.royalsocietypublishing.org

by the shock wave, the state on the left-hand side remains constant during the course of interaction. If the simple wave is not centred but based on data distributed along the axis, one can define the inverse of data as a function of D alone, $\xi(D)$.

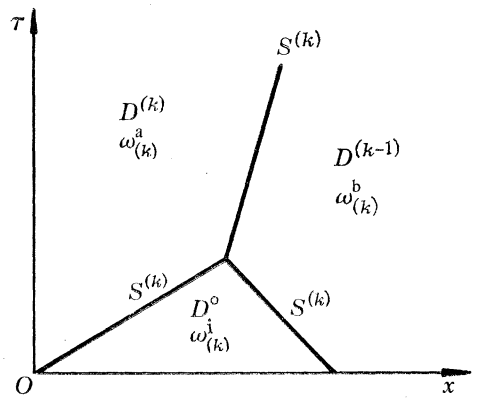

FIGURE 6. Superposition of two (k)-shocks. $D^{(k)} > D^{\circ} > D^{(k-1)}$; $\Lambda_{(k)} = \text{constant}$.

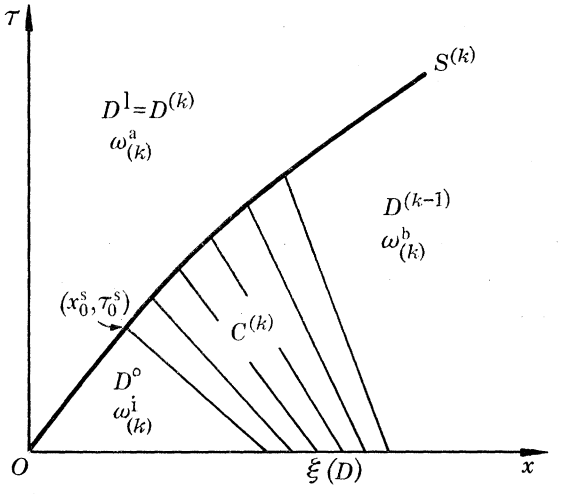

FIGURE 7. Absorption of a (k)-simple wave by a (k)-shock wave. $D^{(k)} > D^{(k-1)} > D^{\circ}$; $\Lambda_{(k)} = \text{constant}$.

Identifying D^{r} with D along the shock line, we obtain the parametric description of the shock line, $S^{(k)}$: $(x^{\mathrm{s}}, \tau^{\mathrm{s}})$, as follows:

$$\tau^{\mathrm{s}} = \sigma_{(k)}(x^{\mathrm{s}} - \xi), \tag{5.2}$$

$$\frac{\mathrm{d}\tau^{\mathrm{s}}}{\mathrm{d}x^{\mathrm{s}}} = \frac{\mathrm{d}\tau^{\mathrm{s}}}{\mathrm{d}D} \Big/ \frac{\mathrm{d}x^{\mathrm{s}}}{\mathrm{d}D} = \sigma^{\mathrm{s}}_{(k)}, \tag{5.3}$$

in which $\mathrm{d}/\mathrm{d}D$ represents differentiation with D as the independent variable along the $\Gamma^{(k)}$ so that $\Lambda_{(k)}$ is held constant. The two equations may be combined in the form

$$(\sigma^{\mathrm{s}}_{(k)} - \sigma_{(k)}) \frac{\mathrm{d}x^{\mathrm{s}}}{\mathrm{d}D} - \frac{\mathrm{d}\sigma_{(k)}}{\mathrm{d}D} x^{\mathrm{s}} = -\frac{\mathrm{d}}{\mathrm{d}D}(\sigma_{(k)}\xi), \tag{5.4}$$

which is a linear differential equation for x^{s} with D as the independent variable. An appropriate initial condition is given by

$$x^{\mathrm{s}} = x^{\mathrm{s}}_0 \quad \text{at} \quad D = D^{\circ}. \tag{5.5}$$

Note that equation (5.4) is non-singular since $\sigma^{\mathrm{s}}_{(k)} \neq \sigma_{(k)}$.

Downloaded from rsta.royalsocietypublishing.org

Substituting equations (2.13) and (2.20) into equation (5.4) and rearranging, we obtain

$$\frac{\mathrm{d}}{\mathrm{d}D}\left\{x^{\mathrm{s}}\frac{(D-D^{1})^{2}}{D^{2}-\mu\Lambda_{(k)}}\right\}=-\frac{(D-D^{1})\,(D^{1}D-\mu\Lambda_{(k)})}{(\nu+\mu)\,\Lambda_{(k)}D}\frac{\mathrm{d}}{\mathrm{d}D}\left\{\frac{D^{2}+\nu\Lambda_{(k)}}{D^{2}-\mu\Lambda_{(k)}}\xi(D)\right\}. \tag{5.6}$$

Direct integration from $D=D^{\circ}$ yields the solution in the form

$$x^{\mathrm{s}}(D;\Lambda_{(k)},D^{1})=x_{0}^{\mathrm{s}}\left(\frac{D^{\circ}-D^{1}}{D-D^{1}}\right)^{2}\frac{D^{2}-\mu\Lambda_{(k)}}{(D^{\circ})^{2}-\mu\Lambda_{(k)}}-\frac{D^{1}}{(\nu+\mu)\,\Lambda_{(k)}}\frac{D^{2}-\mu\Lambda_{(k)}}{(D-D^{1})^{2}}$$
$$\times\left\{(D-D^{1})\left(1-\frac{\mu\Lambda_{(k)}}{D^{1}D}\right)\frac{D^{2}+\nu\Lambda_{(k)}}{D^{2}-\mu\Lambda_{(k)}}\xi(D)\Big|_{D^{\circ}}^{D}-\int_{D^{\circ}}^{D}\left(1+\frac{\nu\Lambda_{(k)}}{D^{2}}\right)\xi(D)\,\mathrm{d}D\right\}, \tag{5.7}$$

where the left-hand side symbolizes that x^{s} is a function of D with $\Lambda_{(k)}$ and D^{1} fixed.

If the (k)-simple wave is centred, we may take the centre as the new origin to put $\xi(D)\equiv 0$, and thus

$$x^{\mathrm{s}}(D;\Lambda_{(k)},D^{1})=x_{0}^{\mathrm{s}}\left(\frac{D^{\circ}-D^{1}}{D-D^{1}}\right)^{2}\frac{D^{2}-\mu\Lambda_{(k)}}{(D^{\circ})^{2}-\mu\Lambda_{(k)}}. \tag{5.8}$$

Otherwise, we shall take the point $(x_{0}^{\mathrm{s}},\tau_{0}^{\mathrm{s}})$ as the origin of the new coordinate system to have $x_{0}^{\mathrm{s}}=\xi(D^{\circ})=0$ and hence

$$x^{\mathrm{s}}(D;\Lambda_{(k)},D^{1})=\frac{D^{1}}{(\nu+\mu)\,\Lambda_{(k)}}\left\{\frac{D^{2}-\mu\Lambda_{(k)}}{(D-D^{1})^{2}}\int_{D^{\circ}}^{D}\left(1+\frac{\nu\Lambda_{(k)}}{D^{2}}\right)\xi(D)\,\mathrm{d}D\right.$$
$$\left.-\left(1-\frac{\mu\Lambda_{(k)}}{D^{1}D}\right)\frac{D^{2}+\nu\Lambda_{(k)}}{D-D^{1}}\xi(D)\right\}. \tag{5.9}$$

The interaction terminates when $D=D^{(k-1)}$.

In the $(k-1)$-intermediate range one may encounter a case when a (k)-shock wave faces a (k)-simple wave on the left-hand side. It is clear that D^{r} remains constant at $D^{(k-1)}$ while D^{1} varies continuously from D° to $D^{(k)}$. Identifying D^{1} with D along the shock line, one can then apply equations (5.7), (5.8), or (5.9) for x^{s} in the form of $x^{\mathrm{s}}(D;\Lambda_{(k)},D^{\mathrm{r}})$.

(*b*) *Transmission*

Here the waves involved are of different kinds and so we shall consider the interaction between a (k)-wave and an (m)-wave, where $k<m$. It can be shown that the image in $\Omega(M)$ falls completely on a single plane parallel to the $\omega_{(k)}$- and $\omega_{(m)}$-axes. It then follows that $\omega_{(l)}$, unless $l=k$ or m, remains constant during the course of interaction. The invariant $\Lambda_{(k)}$, of course, remains unchanged on both sides of the m-wave, whereas $\Lambda_{(m)}$ remains constant on both sides of the (k)-wave.

(i) *Two shock waves*

As shown in figure 8, the interaction is instantaneous and after the interaction the transmitted shocks propagate along straight shock lines of slope

$$\sigma_{(k)}^{\mathrm{s}}=\epsilon\frac{D^{\mathrm{III}}+\nu\omega_{(k)}^{\mathrm{a}}}{D^{\mathrm{III}}-\mu\omega_{(k)}^{\mathrm{a}}} \tag{5.10}$$

and

$$\sigma_{(m)}^{\mathrm{s}}=\epsilon\frac{D^{\mathrm{II}}+\nu\omega_{(m)}^{\mathrm{b}}}{D^{\mathrm{II}}-\mu\omega_{(m)}^{\mathrm{b}}}, \tag{5.11}$$

Downloaded from rsta.royalsocietypublishing.org

respectively. The new constant is characterized by the pair, $\omega^{a}_{(k)}$ and $\omega^{b}_{(m)}$, and given by

$$D^{IV} = D^{II}\omega^{i}_{(m)}/\omega^{b}_{(m)} = D^{III}\omega^{i}_{(k)}/\omega^{a}_{(k)}. \tag{5.12}$$

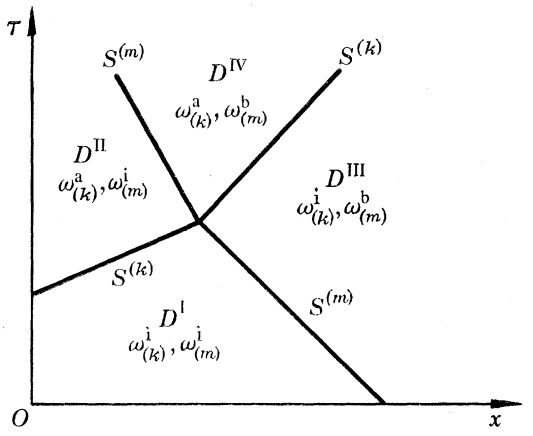

FIGURE 8. Transmission between two shock waves.

(ii) *Pair of a simple wave and a shock wave*

When a (k)-simple wave transmits across an (m)-shock wave from the left-hand side to the right, the physical plane portrait may be given as shown in figure 9. If the simple wave is not centred but based on data distributed along the axis, we can define the inverse of data as a function of D alone, $\xi(D)$.

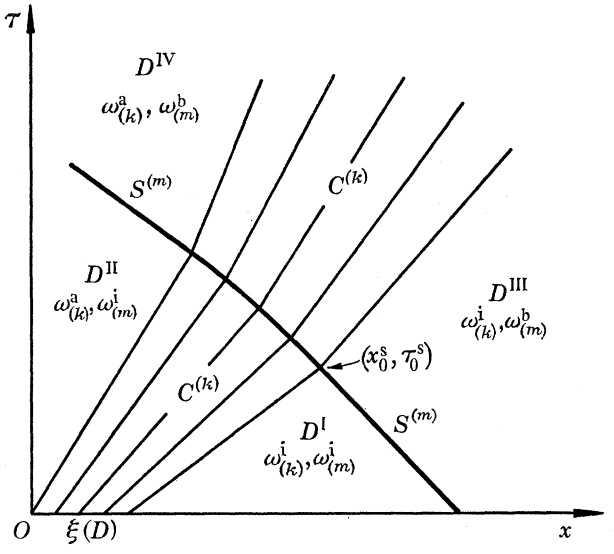

FIGURE 9. Transmission between a simple wave and a shock wave.

We shall identify D^{I} with D along the shock line and denote the differentiation with D as the independent variable along the $\Gamma^{(k)}$ by $\mathrm{d}/\mathrm{d}D$. This implies that both $\Lambda_{(k)}$ and $\omega_{(m)}$ are held constant in the differentiation. It then follows that, along the shock line $S^{(m)}$: (x^{s}, τ^{s}), we have the one-parameter description

$$\tau^{s} = \sigma^{I}_{(k)}(x^{s} - \xi) \tag{5.13}$$

$$\frac{\mathrm{d}\tau^{s}}{\mathrm{d}x^{s}} = \frac{\mathrm{d}\tau^{s}}{\mathrm{d}D}\Big/\frac{\mathrm{d}x^{s}}{\mathrm{d}D} = \sigma^{s}_{(m)}, \tag{5.14}$$

Downloaded from rsta.royalsocietypublishing.org

where both $\sigma^{\mathrm{l}}_{(k)}$ and $\sigma^{\mathrm{s}}_{(m)}$ are functions of D alone. Combining the two equations, we obtain a linear differential equation for x^{s}

$$(\sigma^{\mathrm{s}}_{(m)}-\sigma^{\mathrm{l}}_{(k)})\frac{\mathrm{d}x^{\mathrm{s}}}{\mathrm{d}D}-\frac{\mathrm{d}\sigma^{\mathrm{l}}_{(k)}}{\mathrm{d}D}x^{\mathrm{s}}=-\frac{\mathrm{d}}{\mathrm{d}D}(\sigma^{\mathrm{l}}_{(k)}\xi) \tag{5.15}$$

with the initial condition $$x^{\mathrm{s}}=x^{\mathrm{s}}_0 \quad \text{at} \quad D=D^{\mathrm{I}}. \tag{5.16}$$

By introducing equations (2.13) and (2.22) equation (5.15) can be rewritten in the form

$$\frac{\mathrm{d}}{\mathrm{d}D}\left\{x^{\mathrm{s}}\frac{(D-\Lambda^{\mathrm{l}}_{(k)}/\omega^{\mathrm{b}}_{(m)})^2}{D^2-\mu\Lambda^{\mathrm{l}}_{(k)}}\right\}=-\frac{(D-\Lambda^{\mathrm{l}}_{(k)}/\omega^{\mathrm{b}}_{(m)})\,(D-\mu\omega^{\mathrm{b}}_{(m)})}{(\nu+\mu)\omega^{\mathrm{b}}_{(m)}D}\frac{\mathrm{d}}{\mathrm{d}D}\left\{\frac{D^2+\nu\Lambda^{\mathrm{l}}_{(k)}}{D^2-\mu\Lambda^{\mathrm{l}}_{(k)}}\xi(D)\right\}. \tag{5.17}$$

We then integrate equation (5.17) directly from $D=D^{\mathrm{I}}$ to determine the solution in the form

$$\begin{aligned}x^{\mathrm{s}}(D;\Lambda^{\mathrm{l}}_{(k)},\omega^{\mathrm{b}}_{(m)})=x^{\mathrm{s}}_0&\left(\frac{D^{\mathrm{I}}-\Lambda^{\mathrm{l}}_{(k)}/\omega^{\mathrm{b}}_{(m)}}{D-\Lambda^{\mathrm{l}}_{(k)}/\omega^{\mathrm{b}}_{(m)}}\right)^2\frac{D^2-\mu\Lambda^{\mathrm{l}}_{(k)}}{(D^{\mathrm{I}})^2-\mu\Lambda^{\mathrm{l}}_{(k)}}\\&-\frac{1}{(\nu+\mu)\,\omega^{\mathrm{b}}_{(m)}}\frac{D^2-\mu\Lambda^{\mathrm{l}}_{(k)}}{(D-\Lambda^{\mathrm{l}}_{(k)}/\omega^{\mathrm{b}}_{(m)})^2}\left\{(D-\Lambda^{\mathrm{l}}_{(k)}/\omega^{\mathrm{b}}_{(m)})\left(1-\frac{\mu\omega^{\mathrm{b}}_{(m)}}{D}\right)\frac{D^2+\nu\Lambda^{\mathrm{l}}_{(k)}}{D^2-\mu\Lambda^{\mathrm{l}}_{(k)}}\xi(D)\right|^{D}_{D^{\mathrm{I}}}\\&-\int_{D^{\mathrm{I}}}^{D}(1+\nu\Lambda^{\mathrm{l}}_{(k)}/D^2)\,\xi(D)\,\mathrm{d}D\Bigg\}\end{aligned} \tag{5.18}$$

in which D is the independent variable and both of $\Lambda^{\mathrm{l}}_{(k)}$ and $\omega^{\mathrm{b}}_{(m)}$ are fixed parameters.

If the (k)-simple wave is centred, we can put $\xi(D)\equiv 0$ to obtain

$$x^{\mathrm{s}}(D;\Lambda^{\mathrm{l}}_{(k)},\omega^{\mathrm{b}}_{(m)})=x^{\mathrm{s}}_0\left(\frac{D^{\mathrm{I}}-\Lambda^{\mathrm{l}}_{(k)}/\omega^{\mathrm{b}}_{(m)}}{D-\Lambda^{\mathrm{l}}_{(k)}/\omega^{\mathrm{b}}_{(m)}}\right)^2\frac{D^2-\mu\Lambda^{\mathrm{l}}_{(k)}}{(D^{\mathrm{I}})^2-\mu\Lambda^{\mathrm{l}}_{(k)}}. \tag{5.19}$$

Otherwise, we may translate the coordinate axes so that the point $(x^{\mathrm{s}}_0,\tau^{\mathrm{s}}_0)$ should become the origin. Since then $x^{\mathrm{s}}_0=\xi(D^{\mathrm{I}})=0$, it follows from equation (5.18) that

$$\begin{aligned}x^{\mathrm{s}}(D;\Lambda^{\mathrm{l}}_{(k)},\omega^{\mathrm{b}}_{(m)})=\frac{1}{(\nu+\mu)\,\omega^{\mathrm{b}}_{(m)}}&\left\{\frac{D^2-\mu\Lambda^{\mathrm{l}}_{(k)}}{(D-\Lambda^{\mathrm{l}}_{(k)}/\omega^{\mathrm{b}}_{(m)})^2}\int_{D^{\mathrm{I}}}^{D}(1+\nu\Lambda^{\mathrm{l}}_{(k)}/D^2)\,\xi(D)\,\mathrm{d}D\right.\\&\left.-\left(1-\frac{\mu\omega^{\mathrm{b}}_{(m)}}{D}\right)\frac{D^2+\nu\Lambda^{\mathrm{l}}_{(k)}}{D-\Lambda^{\mathrm{l}}_{(k)}/\omega^{\mathrm{b}}_{(m)}}\xi(D)\right\}.\end{aligned} \tag{5.20}$$

The interaction terminates when $D=D^{\mathrm{II}}$.

By applying the invariant $\Lambda_{(m)}$ across the (m)-shock and the invariant $\Lambda^{\mathrm{l}}_{(k)}$ on the left-hand side we can determine the state on the right-hand side in the form

$$D^{\mathrm{r}}=\frac{\omega^{\mathrm{i}}_{(m)}}{\omega^{\mathrm{b}}_{(m)}}D^{\mathrm{l}}=\left(\frac{\omega^{\mathrm{i}}_{(m)}}{\omega^{\mathrm{b}}_{(m)}}\Lambda^{\mathrm{l}}_{(k)}\right)\frac{1}{\omega_{(k)}} \quad \text{for} \quad \omega^{\mathrm{i}}_{(k)}\leqslant\omega_{(k)}\leqslant\omega^{\mathrm{a}}_{(k)}. \tag{5.21}$$

Every $C^{(k)}$ is refracted across the (m)-shock due to the jump in the state but the parameter $\omega_{(k)}$ remains invariant along it. Substituting equation (5.21) into equation (2.22), we obtain the slope of the refracted $C^{(k)}$ in terms of the parameter $\omega_{(k)}$:

$$\sigma^{\mathrm{r}}_{(k)}=\epsilon\frac{(\omega^{\mathrm{i}}_{(m)}/\omega^{\mathrm{b}}_{(m)})\,\Lambda^{\mathrm{l}}_{(k)}+\nu\omega^2_{(k)}}{(\omega^{\mathrm{i}}_{(m)}/\omega^{\mathrm{b}}_{(m)})\,\Lambda^{\mathrm{l}}_{(k)}-\mu\omega^2_{(k)}} \quad \text{for} \quad \omega^{\mathrm{i}}_{(k)}\leqslant\omega_{(k)}\leqslant\omega^{\mathrm{a}}_{(k)}. \tag{5.22}$$

The totality of the refracted $C^{(k)}$'s establishes the transmitted (k)-simple wave.

If an (m)-simple wave transmits across a (k)-shock wave from the right-hand side to the left, we can follow the same procedure with appropriate replacements of parameters. In particular, we obtain the (k)-shock line from equation (5.18), (5.19) or (5.20) in the form of $x^{\mathrm{s}}(D;\Lambda^{\mathrm{r}}_{(m)},\omega^{\mathrm{a}}_{(k)})$.

PHILOSOPHICAL TRANSACTIONS OF THE ROYAL SOCIETY A MATHEMATICAL, PHYSICAL & ENGINEERING SCIENCES

PHILOSOPHICAL TRANSACTIONS OF THE ROYAL SOCIETY A MATHEMATICAL, PHYSICAL & ENGINEERING SCIENCES

Downloaded from rsta.royalsocietypublishing.org

(iii) *Two simple waves*

The interaction generates a non-simple and non-shock wave region in the physical plane. Fortunately, however, the image in $\Omega(M)$ falls on the inside of a rectangle surrounded by Γ's as shown in figure 10 (a) for the interaction between a (k)-simple wave and an (m)-simple wave. Two adjacent sides, $\overline{\mathrm{III}}$ and $\overline{\mathrm{IIII}}$, represent the image before interaction while the other two denote the image after interaction.

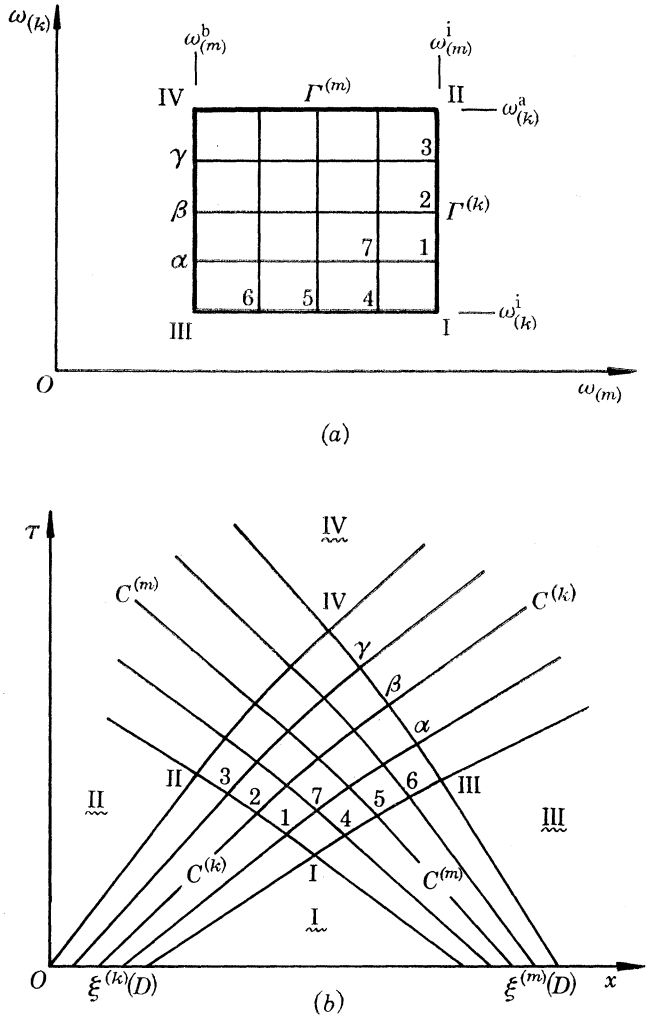

FIGURE 10. Transmission between two simples waves. (a) Image in $\Omega(M)$. (b) Physical plane portrait.

The solution is then determined by mapping the image in $\Omega(M)$ onto the physical plane. Since for the present case $\omega_{(k)}$ and $\Lambda_{(m)}$ remain constant along a $C^{(k)}$, whereas $\omega_{(m)}$ and $\Lambda_{(k)}$ remain constant along a $C^{(m)}$, the mapping can be readily performed by employing the characteristics, $C^{(k)}$ and $C^{(m)}$. A schematic portrait in the physical plane is shown in figure 10 (b), in which the correspondence to figure 10 (a) is illustrated with 25 points. The procedure of mapping is briefly discussed in the following:

First we introduce an appropriate network to the image in $\Omega(M)$ and read the values of $\omega_{(k)}$ and $\omega_{(m)}$ at each mesh point. By applying the (k)- or (m)-Riemann invariants we also determine

Downloaded from rsta.royalsocietypublishing.org

the parameter D and the state $\{c_i\}$ corresponding to each mesh point. The values of $\sigma_{(k)}$ and $\sigma_{(m)}$ are evaluated by using equation (2.12) at each mesh point.

In the physical plane the curved portions $\widehat{\mathrm{I\,II}}$ and $\widehat{\mathrm{I\,III}}$ are obtained by applying equation (5.18) in the form of $x^{\mathrm{s}}(D; A^{\mathrm{I}}_{(k)}, \omega^{\mathrm{i}}_{(m)})$ for $\widehat{\mathrm{I\,II}}$ and of $x^{\mathrm{s}}(D; A^{\mathrm{I}}_{(m)}, \omega^{\mathrm{i}}_{(k)})$ for $\widehat{\mathrm{I\,III}}$, respectively. In the region of interaction the portion $\widehat{1\,7}$ of a $C^{(k)}$, for example, may be approximated by a straight line of slope.

$$\sigma_{(k)} = \tfrac{1}{2}(\sigma^{1}_{(k)} + \sigma^{7}_{(k)}) \tag{5.23}$$

and the portion $\widehat{4\,7}$ of a $C^{(m)}$ can be drawn likewise to yield the point 7 at the intersection. Iteration completes the mapping and generates the non-simple wave solution in the region, I II IV III. The more mesh points we use, the more accurate solution can be obtained.

The transmitted (k)-simple wave is established by drawing a straight $C^{(k)}$ from each of the points III, α, β, γ, and IV with the slope $\sigma_{(k)}$ given at the point. The same holds for the transmitted (m)-simple wave.

6. Application

In order to illustrate applications of the theory developed we shall consider a numerical example involved with three solutes in a finite column. The entry fluid phase contains A_1, A_2 and A_3 in the same amount while the incoming solid phase is half saturated by the most strongly adsorbable solute A_3 alone. Concentrations are expressed in moles per litre of individual phase. The parameters and the initial and entry data are given as follows:

$\epsilon = 0.4, \quad N = 1.0;$

	$m = 1$	2	3	D	Θ
K_m	5.0	10.0	15.0	—	—
c^{a}_m	0.05	0.05	0.05	2.5	—
c^{i}_m	0.025	0.036	0.075	2.61	0.6168
n^{b}_m	0	0	0.5	—	0.5
$\omega^{\mathrm{a}}_{(m)}$	3.387	7.050	12.563	—	—
$\omega^{\mathrm{i}}_{(m)}$	3.803	6.516	11.597	—	—
$\omega^{\mathrm{b}}_{(m)}$	5.0	7.5	10.0	—	—

The set $\{\omega_{(m)}\}$ is determined by solving equation (2.7) for the corresponding data with the equilibrium relation (2.1).

(i) *Ranges of μ*

Critical values of μ are evaluated by applying equations (4.1) and (4.5) or (4.6) to determine various ranges of μ:

lower range	$0 \leqslant \mu < 0.199$
(3)-transition range	$0.199 \leqslant \mu \leqslant 0.314$
(2)-intermediate range	$0.314 < \mu < 0.419$
(1)-intermediate range	$0.419 \leqslant \mu < 0.591$
upper range	$0.591 \leqslant \mu < \infty.$

(ii) *Steady state*

There are four different steady states attainable within the domain and these are independent of the initial data. These states are determined by applying equation (4.2) and presented in the following table.

Downloaded from rsta.royalsocietypublishing.org

	$m = 1$	2	3	D	remark
c_m^a	0.05	0.05	0.05	2.5	lower range
$c_m^{(2)}$	0.0415	0	0.1289	3.141	(2)-intermediate range
$c_m^{(1)}$	0.0476	0	0.1143	2.953	(1)-intermediate range
$c_{m,\mathrm{eq}}^b$	0	0	0.0667	2.0	upper range

The states of the outgoing phases are readily obtained by applying equations (1.22) and (1.23) if the parameter μ is given. Hence the steady-state coverage of the outgoing solid phase can be evaluated for various values of μ as presented in figure 11. The maximum coverage gain is attained when $\mu = \mu^{s(1)} = 0.591$.

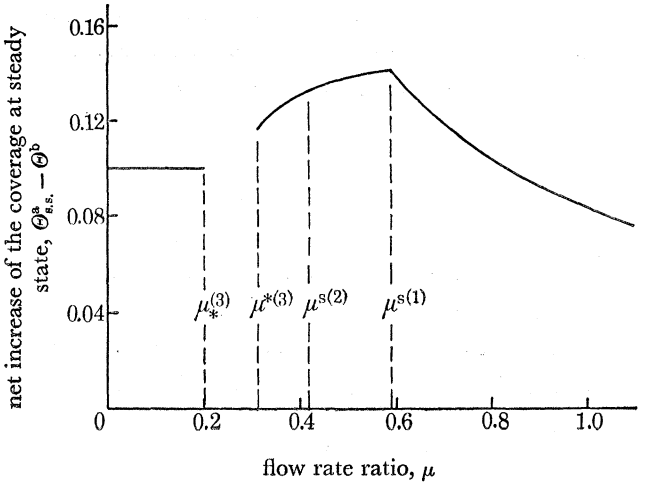

FIGURE 11. Coverage gain at steady state as a function of μ.

(iii) *Solution for* $\mu = 0.36$

Two transmissive interactions are involved and analyses are performed by applying the result of the previous section. Figure 12 shows the physical plane portrait of the solution. The constant state $\underset{\sim}{I}^{\mathrm{i}}$ is the initial state and the state $\underset{\sim}{(k)}$ corresponds to the (k)-constant state. The other constant states are given in the following:

constant state	c_1	c_2	c_3	D
I	0.0378	0.0431	0.0873	2.93
II	0.0472	0.0337	0.0756	2.708
III	0.0220	0	0.1278	3.027
IV	0.0332	0	0.1488	3.398
V	0.0316	0	0.0980	2.628

Since in figure 12 the values of $\omega_{(m)}$ are given appropriately, one can determine the state along each characteristic (even through the non-simple wave region) by applying equation (2.8) or the pertinent Riemann invariants. The result is presented in figure 13 in the form of concentration profiles at five different times. The arrow represents the propagation direction of the corresponding wave and here the interaction phenomena are better visualized. Both boundary discontinuities are shown. The non-simple wave solution in this particular example indicates that the (3)-simple wave is dominant over the (2)-simple wave in the interaction.

Downloaded from rsta.royalsocietypublishing.org

At $\tau = 18.52$, the operation reaches a steady state and this state is given by equation (4.9) for $k = 2$. At this steady state 64.6% of A_1 and 100 % of A_2 are adsorbed from the entry mixture while 20.7 % of A_3 is desorbed from the incoming solid phase. The coverage increases from 0.5 to 0.6252.

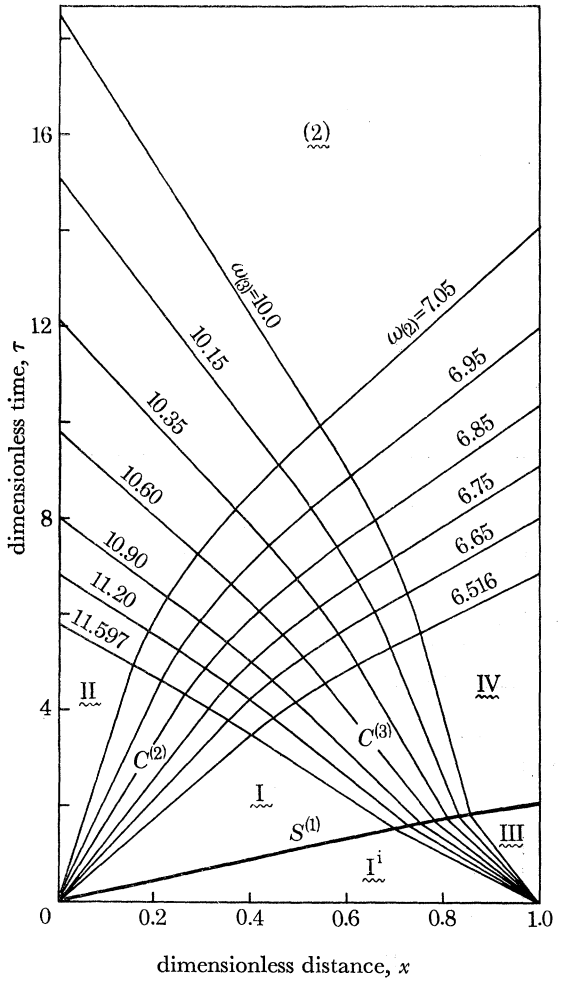

FIGURE 12. Physical plane portrait of the solution for $\mu = 0.36$. $\omega_{(1)} = 3.387$ above $S^{(1)}$; 3.803 below $S^{(1)}$.

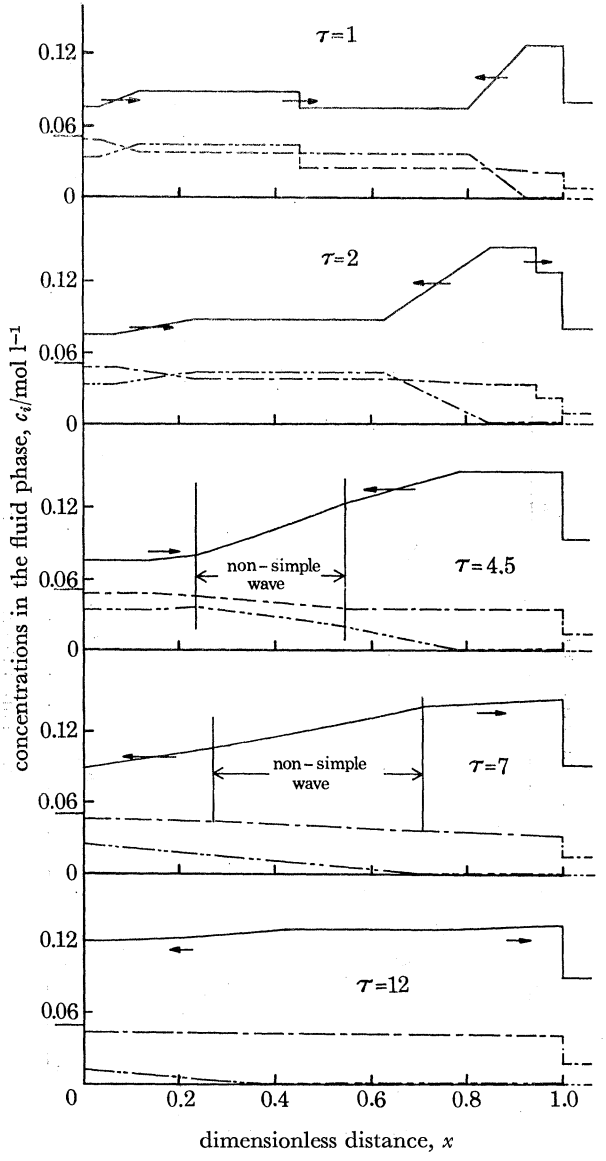

FIGURE 13. Distribution of solutes for $\mu = 0.36$. — · —, Solute A_1; — · · —, solute A_2; ——, solute A_3; →, propagation direction.

(iv) *Solution for* $\mu = 0.54$

Two transmissive interactions and one superposition are analysed to generate the physical plane portrait as shown in figure 14. Note that the constant state E^b of the entry data appears for $\tau < 5.0$ so that the boundary $\mathscr{B}^b$ remains continuous meanwhile. The other constant states were given in the previous subsection.

Figure 15 shows the distribution of solutes at five different times. Since the propagation

Downloaded from rsta.royalsocietypublishing.org

directions are indicated by arrows, one can see the interacting wave pairs and the processes of interaction.

At $\tau = 7.67$ the operation attains a steady state and the state is given by equation (4.9) for $k = 1$. Here 7.62 % desorption of A_3 is accompanied by 91.8 % adsorption of A_1 and 100 % adsorption of A_2 from the entry mixture. The adsorption yield is improved from that for $\mu = 0.36$.

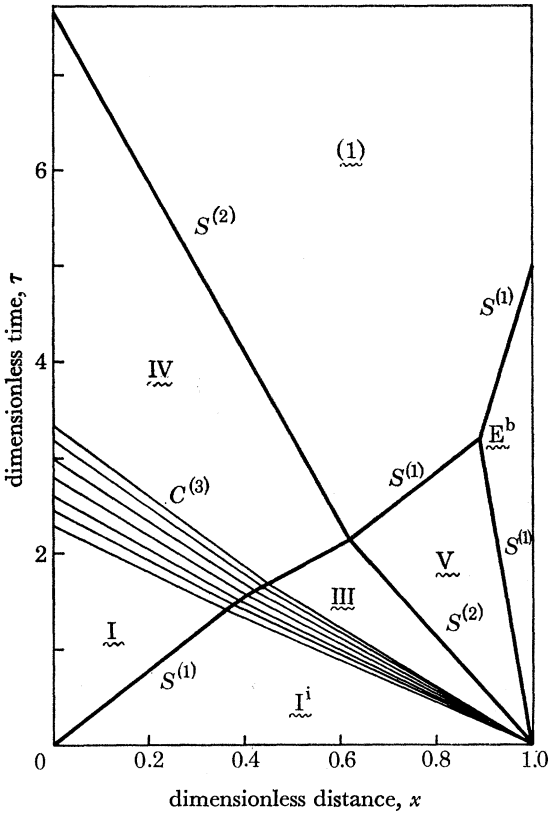

FIGURE 14. Physical plane portrait of the solution for $\mu = 0.54$.

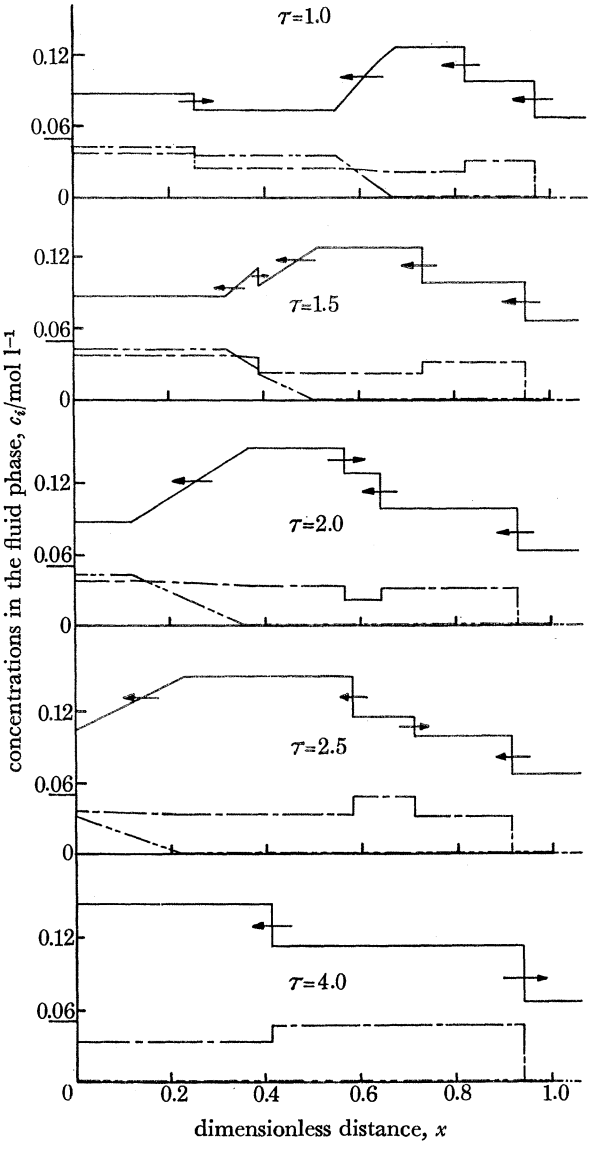

FIGURE 15. Distribution of solutes for $\mu = 0.54$. — - —, Solute A_1; — - - —, solute A_2; ——, solute A_3; →, propagation direction.

As we pointed out previously, the coverage reaches the maximum when $\mu = 0.591$ and, correspondingly, the maximum adsorption yield is achieved. The superposed (1)-shock then becomes stationary at $x = 0.83$ when $\tau = 3.32$ and the steady state is attained when $\tau = 4.83$. Otherwise the physical plane portrait is analogous to figure 14. In contrast to the 5.56% desorption of A_3, 100 % adsorption of both A_1 and A_2 from the entry mixture is achieved.

Downloaded from rsta.royalsocietypublishing.org

References

Courant, R. & Friedrichs, K. O. 1948 *Supersonic flow and shock waves*. New York: Interscience.
Heerdt, E. D. 1969 Ph.D. Thesis, *University of Minnesota*.
Helfferich, F. 1968 *Advances in chemistry series*, no. **79**, 30.
Lax, P. D. 1957 *Communs. pure Appl. Math.* **10**, 537.
Rhee, H., Aris, R., & Amundson, N. R. 1970 *Phil. Trans. Roy Soc. Lond.* A. **267**, 419.
Treybal, R. E. 1968 *Mass transfer operations*, 2nd ed. New York: McGraw-Hill.

PHILOSOPHICAL TRANSACTIONS OF THE ROYAL SOCIETY A MATHEMATICAL, PHYSICAL & ENGINEERING SCIENCES

PHILOSOPHICAL TRANSACTIONS OF THE ROYAL SOCIETY A MATHEMATICAL, PHYSICAL & ENGINEERING SCIENCES